Water Research 222 (2022) 118907

Contents lists available at ScienceDirect

Water Research

journal homepage: www.elsevier.com/locate/watres

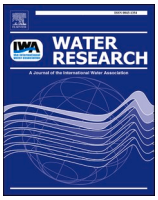

Lake metabolic processes and their effects on the carbonate weathering CO_2 sink: Insights from diel variations in the hydrochemistry of a typical karst lake in SW China

Haibo He [a,b], Yuyouting Wang [c], Zaihua Liu [a,d,*], Qian Bao [a,e], Yu Wei [a], Chongying Chen [a], Hailong Sun [a]

[a] State Key Laboratory of Environmental Geochemistry, Institute of Geochemistry, Chinese Academy of Sciences (CAS), 99 Lincheng West Road, Guiyang 550081, China
[b] Yunnan Key Laboratory of Earth System Science, Yunnan University, Kunming 650500, China
[c] Yunnan Climate Center, Kunming 650034, China
[d] CAS Center for Excellence in Quaternary Science and Global Change, Xi'an 710061, China
[e] Key Laboratory of Land Resources Evaluation and Monitoring in Southwest China of Ministry of Education, Sichuan Normal University, Chengdu 610066, China

ARTICLE INFO

Keywords:
Carbonate weathering-related carbon sink
Lake metabolism
Aquatic phototrophs
Diel monitoring
Carbon cycling
Net ecosystem production

ABSTRACT

The precipitation of carbonate minerals does not invariably result in CO_2 emission to the atmosphere, because dissolved inorganic carbon (DIC) can be partially utilized by terrestrial aquatic phototrophs, thus generating an autochthonous organic carbon (AOC) sink. However, little is known about the potential effects of this mechanism on carbon cycles in DIC-rich lakes, mainly due to the lack of detailed documentation of the related processes, which limits our ability to accurately evaluate and predict the magnitude of this carbon sink. We conducted field observations in Fuxian Lake, a large and representative karst lake in the Yunnan-Guizhou Plateau, SW China. Continuous diel monitoring was conducted to quantitatively assess the coupled relationship between lake metabolism and DIC cycling and its influence on the carbonate weathering-related CO_2 sink. We found that the diel physicochemical variations and isotopic characteristics were mainly controlled by the metabolism of aquatic phototrophs, evidenced by a significant relationship between net ecosystem production and diel DIC cycling, and demonstrating the significance of DIC fertilization in supporting high primary production in karst lakes. The data showed that a reduction in photosynthesis occurred in the afternoon of almost every day, which can be explained by the lower CO_2/O_2 ratio that increased the potential for the photorespiration of aquatic plants, thus reducing photosynthesis. We found that a net autotrophic ecosystem prevailed in Fuxian Lake, suggesting that the lake functions more as a sink than a source of atmospheric CO_2. Considering carbonate weathering, the estimated AOC sink amounted to 650–704 t C km^{-2} yr^{-1}, demonstrating both the potentially significant role of metabolism in lacustrine carbon cycling and the potential of the combination of photosynthesis and carbonate weathering for carbon sequestration. Our findings may help to quantitatively estimate the future impact of lake metabolism on carbon cycling, with implications for formulating management policies needed to regulate the magnitude of this carbon sink.

1. Introduction

Primary energy demand fell by almost 4% in 2020 and global energy-related CO_2 emissions fell by 5.8%, according to the latest statistical data from the International Energy Agency. Although this was the largest annual percentage decline since World War II, the emissions still reached a monitored 31.5 billion metric tons, which far exceeds the 20.5 billion metric tons in 1990 (https://www.iea.org/), and the resulting global warming has been a focus of concern amongst academics and governments (Regnier et al., 2013; Beerling et al., 2020; Goll et al., 2021). Pertinent to the climate crisis, in addition to artificial carbon capture and storage technology, several natural physicochemical and biological processes in nature, such as rock weathering and photosynthesis, can also capture and store atmospheric CO_2.

* Corresponding author at: State Key Laboratory of Environmental Geochemistry, Institute of Geochemistry, Chinese Academy of Sciences (CAS), 99 Lincheng West Road, Guiyang 550081, China.
E-mail address: liuzaihua@vip.gyig.ac.cn (Z. Liu).

https://doi.org/10.1016/j.watres.2022.118907
Received 7 April 2022; Received in revised form 10 July 2022; Accepted 23 July 2022
Available online 25 July 2022

In recent years, the view that the carbon fixed by the coupling of carbonate weathering and aquatic photosynthesis can represent an important global carbon sink has attracted increasing research interest (Liu et al., 2010, 2011, 2017, 2018, 2021, 2015; Yang et al., 2015; He et al., 2019, 2020, 2021a; Chen et al., 2017, 2021; Pu et al., 2017; Bao et al., 2022; Sun et al., 2022). Carbonate weathering liberates base cations and provides abundant dissolved inorganic carbon (DIC) which is converted from atmospheric CO_2 (Zeng et al., 2022) and can subsequently be utilized by aquatic photosynthesis as a carbon source during biological carbon pumping (BCP) in aquatic environments (Zhao et al., 2022). The generated autochthonous organic carbon (AOC) is the product of the transformation of DIC to organic carbon (OC), which plays an underestimated role in climate change on various timescales (Liu et al., 2010, 2018, 2021). Whether carbonate weathering can provide a significant and sustained carbon sink, in which the utilization of DIC by aquatic phototrophs cannot be ignored (Liu et al., 2010, 2011, 2018, 2021; Yang et al., 2015; Liu et al., 2015; Chen et al., 2017), can be investigated by determining the diel variations in lake metabolic processes and carbon cycling in lake surface waters. However, such studies are relatively rare.

Clarifying the origin, evolution and dynamic processes involving DIC is crucial to advancing our understanding of the carbon cycling in karst aquatic ecosystems and its role in regional and global carbon budgets (Pu et al., 2017). The dynamics of biogeochemical cycles, including carbon cycles in aquatic ecosystems, are related to metabolic processes involving the production or utilization of organic matter. Lakes with high primary productivity typically show substantial deceases in DIC and increases in dissolved oxygen (DO) during the day, with the opposite trends at night, in response to changes in photosynthesis and respiration by aquatic plants (Nimick et al., 2011). These changes, coupled with those of water temperature, may result in diel-scale variations in nutrients and other physical, chemical and isotopic species. Previous research has emphasized specific aspects of the biochemistry of karst waters, focusing mainly on the effects of aquatic metabolism on carbon cycling (Jiang et al., 2013; Yang et al., 2015; Liu et al., 2015; Chen et al., 2017; He et al., 2019). However, much of the relevant literature is qualitative and a comprehensive and quantitative study of aquatic metabolism and its role in carbon cycling has rarely been attempted for lake ecosystems.

Lake metabolism is a key factor for understanding the carbon and energy transfers to, from, and within lake ecosystems (Odum, 1956; Aho et al., 2021; Castro et al., 2021; Herrera and Nadaoka, 2021). Observations of the production and respiration of marine plankton communities have promoted studies aimed to determine whether aquatic ecosystems act as sinks or sources of atmospheric CO_2 via estimating the net autotrophic or heterotrophic balance, and this analytical approach was later extended to lakes (e.g., Broecker et al., 1979; Cole et al., 1994; Duarte and Agusti, 1998). The metabolism of aquatic ecosystems is often expressed in terms of the gross primary production (GPP) and ecosystem respiration (R), which can help evaluate the metabolic balance of ecosystems and assess their roles in autotrophic or heterotrophic systems (Gazeau et al., 2005; Hu et al., 2015). GPP and R together represent the metabolic balance of aquatic ecosystems, termed the net ecosystem production (NEP=GPP−R), which provides information about the sources or sinks of atmospheric CO_2. For example, when GPP>R (NEP>0), aquatic photoautotrophs can effectively transfer DIC to OC, while when GPP<R (NEP<0), the consumption of OC exceeds the production (Odum, 1956; Solomon et al., 2013; Castro et al., 2021). It is currently assumed that lakes worldwide are usually net heterotrophic (GPP<R) and supersaturated with CO_2 due to the inputs of allochthonous carbon (e.g., Cole et al., 1994, 2007; Duarte and Agusti, 1998). However, evidence of the net heterotrophic status of these lakes is derived using different methods, and the methods used to estimate metabolism and the range of lake types studied are limited. Especially, dissolved organic carbon (DOC) and total phosphorus (TP) are important factors that have been used to draw different conclusions (Cole et al., 2000; Prairie et al., 2002; Hanson et al., 2003). For instance, contrary to previous estimates for lakes worldwide, 60% of eutrophic lakes were undersaturated with respect to CO_2 (Michelle and John, 2011). Moreover, lake metabolism is controlled by different physical, chemical, and biological parameters, such as temperature, pH, wind speed, solar radiation, nutrients, biomass, and community structure (Duarte and Agustí, 1998; Cole et al., 2000; Prairie et al., 2002; Hanson et al., 2003; Amaral et al., 2018; Herrera and Nadaoka, 2021). Additionally, detailed and fine-scale monitoring, such as of lake metabolism on the diel scale (Staehr et al., 2012), is important for reducing the uncertainty of heterotrophic versus autotrophic assessments of lakes.

Our focus in this study is on terrestrial carbonate rock weathering coupled with aquatic photosynthesis, which is an atmospheric CO_2 removal mechanism, given the need to better understand the variability and magnitude of this carbon sink (Liu et al., 2018). Since global changes are expected to affect the intensity of carbonate weathering, water level, temperature, illumination, and the degree of eutrophication, the increased recognition of lake metabolism is needed to better understand the capacity of the carbon sink associated with carbonate weathering in terrestrial aquatic ecosystems. However, the current limited sampling involved in carbon budget calculations, and the inherent fine-scale variations of these processes, make estimating the carbon sink for terrestrial aquatic ecosystem extremely challenging.

In this study, climatic and biochemical parameters (GPP, R, and NEP) were calculated using intensive diel observations, quarterly, and throughout a full year, in the northern and southern parts of Fuxian Lake, a large and representative karst lake in Yunnan, SW China, using various data logging sensors and water sampling. We quantitatively assess the role of lake metabolism in carbon cycling using a bookkeeping metabolism model. Further, we compare the GPP and R to determine whether the aquatic ecosystem of Fuxian Lake acts as a net CO_2 source or sink. If the ecosystem is a sink, especially relating to carbonate weathering, the question arises regarding the magnitude of the sink flux. The answers to these questions can potentially provide insights into the role of metabolism in the evolution of the lake carbon cycle, in the context of quantifying atmospheric CO_2 removal via the interaction between carbonate weathering and aquatic phototrophs, and to better understand the terrestrial carbon sink.

2. Materials and methods

2.1. Site description

Fuxian Lake (24°21′–24°37′N, 102°49′–102°57′E; 1722.5 m above sea level) is a large and deep lake (area: 212 km^2; maximum depth: 158.9 m; mean depth: 95.2 m; volume: 20.62×10^9 m^3) in the Yunnan-Guizhou Plateau in Yunnan Province, Southwest China (Fig. 1). It is the second deepest freshwater lake in China. The catchment area is relatively small (675 km^2), with more than 20 short streams entering the lake. The lake has a wide and deep northern basin and a comparatively narrow and shallow southern basin. It is a karst faulted lake, with a large distribution of limestone exposure that represents ~60% of the catchment area and thus its hydrochemistry is dominated by HCO_3–Ca–Mg (He et al., 2019). It is oligotrophic with long-term annual values of total phosphorus (TP) of 0.005 to 0.013 mg L^{-1}, total nitrogen (TN) of 0.100 to 0.223 mg L^{-1}, chlorophyll-a of 0.16 to 2.34 μg L^{-1} (1986–2015), and water transparency of ~5 m (Zhang et al., 2021). The average annual precipitation within the Fuxian Lake basin is 951 mm, and the annual mean temperature is 15.6 °C. The diversity and species richness of the phytoplankton in Fuxian Lake are low; the lake biota are mainly green algae, followed by cyanobacteria, diatoms and dinoflagellates (Li et al., 2007). Submerged plants in Fuxian Lake are mainly distributed in the shallow water area (5.1 km^2) along the lake margin, in depths of 0.5–14 m (4.3 m on average) and accounting for 2.4% of the lake surface. Phytoplankton are the major primary producers in Lake Fuxian (Zhang et al., 2021). There are almost no emergent and floating leaf plant

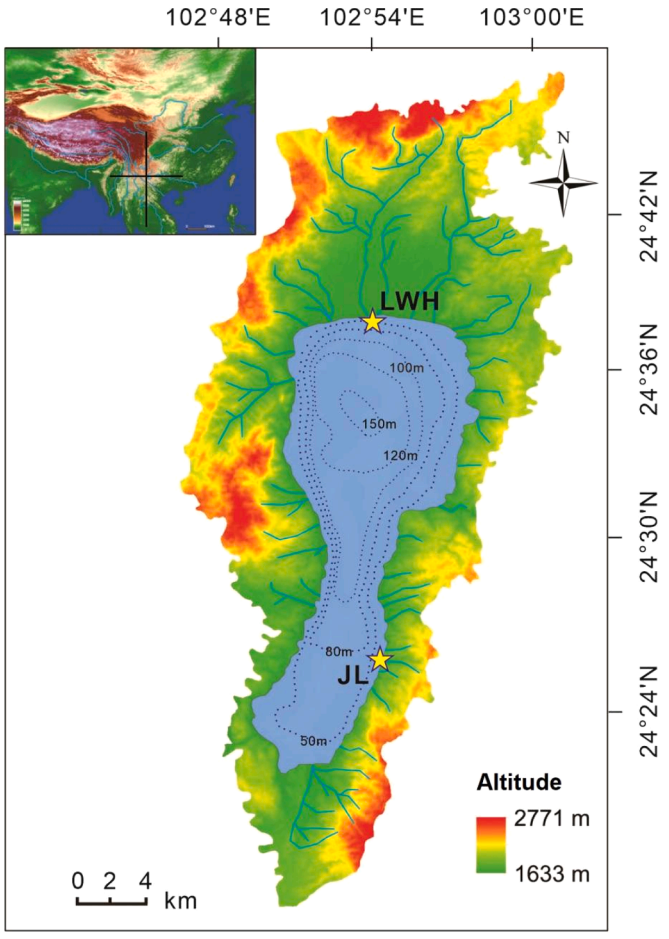

Fig. 1. Location of Fuxian Lake and the sampling sites. LWH, and JL are monitoring sites in the northern and southern sectors of the lake, respectively. The basin boundary and bathymetry are from Liu et al. (2008).

communities in the lake, and the dominant submerged plants are Characean algae, *Myriophyllum spicatum, Vallisneria natans, Potamogeton pectinatus*, and *Ceratophylum demersum* (He and Li, 2021). In recent years, although the total biomass and spatial distribution of submerged plants have increased substantially, the lake ecosystem has not exceeded a tipping point. The lake has never been considered to be a eutrophic lake (water quality: type I) (Li et al., 2007; Liu et al., 2008; He and Li, 2021), which is also reflected by molecular sedimentary evidence over the past century (Zhang et al., 2021; He et al., 2021b).

2.2. Data acquisition

Given the importance of the diel dynamics in subtropical water bodies, we intensively monitored various lake physicochemical variables during both the day and night. Data and samples were collected in the lake margins in the northern and southeastern parts of Fuxian Lake (LWH and JL, respectively) (Fig. 1), at the depth of 50 cm. Continuous measurements over 24–49 h were made of meteorological and physicochemical variables to understand the diel dynamics of Fuxian Lake in winter (January 17–18), spring (April 21–23), summer (July 27–29), and autumn (October 29–31), under stable meteorological conditions, without precipitation events, during 2017. Two hand-held water quality meters (PONSEL ODEN, France) were programmed to measure temperature (T), pH, electrical conductivity (EC, 25°C), and dissolved oxygen (DO) at 15 min intervals spanning a complete diurnal cycle. The meters were calibrated prior to deployment using pH (4, 7 and 10), EC (1413 μs cm^{-1}), and DO (0%, = 100%) standards. The resolutions of the measurements of T, pH, EC, and DO are 0.01°C, 0.01, 0.1 μs cm^{-1} and 0.01 mg L^{-1}, respectively. An on-site meteorological station provided observations of atmospheric temperature, relative humidity, evaporation capacity, precipitation, wind velocity and direction, and solar radiation at 60 min intervals.

Water samples were collected every two hours during the day and every four hours at night. Two sets of water samples for measuring major cations (Ca^{2+}, Mg^{2+}, K^+ and Na^+) and anions (Cl^-, SO_4^{2-} and NO_3^-) were filtered in the field using 0.45 μm Millipore nitrocellulose filters, and 20 ml of these samples were stored in acid-washed HDPE bottles. Cation samples were acidified to pH<2 using concentrated ultrapure HNO_3, and no preservatives were added to the samples collected for major anions. Both cationic and anionic samples were stored in a refrigerator at 4 °C. Major anions were analyzed using an automated Dionex ICS-90 ion chromatograph (Dionex, USA), and major cations were analyzed using an inductively coupled plasma optical emission spectrometer (ICP-OES, USA). Procedural blanks and reagent were measured in parallel with the samples. The detection limit of these ions was 0.01 mg L^{-1}. Additionally, DIC concentrations were titrated *in situ* using an Aquamerck alkalinity test kit (Merck, Germany) with an estimated accuracy of 0.05 mmol L^{-1}. The pH values of the water column ranged from 7.9 to 9.3, and thus the DIC in the water column is dominated by HCO_3^-, which accounts for over 95% of the total (HCO_3^-, dissolved CO_2 (CO_{2aq}), and CO_3^{2-}). Therefore, we used HCO_3^- as an approximation for DIC. Based on the concentrations of Ca^{2+} and Mg^{2+}, as well as the titration of HCO_3^-, regression analysis of the concentrations of these ions and EC was used to estimate the concentrations of Ca^{2+} and HCO_3^- which were used for further calculations (Yang et al., 2015; Liu et al., 2015).

The remaining water samples (60 ml), for $\delta^{13}C_{DIC}$ measurements, were filtered by pressure filtration through 0.45 μm cellulose acetate filters and collected in acid-washed HDPE bottles with air-tight caps, with no air bubbles or headspace. One drop of saturated $HgCl_2$ was added to prevent microbial activity and all samples were stored in a refrigerator at 4 °C. $\delta^{13}C_{DIC}$ values were analyzed using an MAT-253 mass spectrometer with analytical precision typically better than ±0.03‰, based on replicate measurements of an internal laboratory standard. The results are expressed as $\delta^{13}C_{DIC}$ (‰) with respect to the international Vienna Peedee Belemnite (VPDB) standard. All the laboratory analyses were carried out at the State Key Laboratory of Environmental Geochemistry, Chinese Academy of Sciences.

The CO_2 partial pressure (pCO_2) and calcite saturation index (SI_C) are important indicators for karst water chemistry research; however, both are difficult to determine directly using instrumentation and they need to be estimated from model calculations. pCO_2 and SI_C in water were calculated using the hydrogeochemical simulation software PHREEQC Interactive version 3.3.8 (database: phreeqc. dat), which was developed by the United States Geological Survey (USGS) (https://www.usgs.gov/software/phreeqc-version-3). The hydrochemical datasets, including T, pH and the concentrations of K+, Na+, Ca2+, Mg2+, HCO3−, Cl−, SO42− and NO3− were used as inputs. Assuming the pCO_2 in the water body reaches exchange equilibrium with the collected water samples, pCO_2 can be calculated as:

$$pCO_2 = \frac{(HCO_3^-)(H^+)}{K_1 K_{CO_2}} \quad (1)$$

where the species in parentheses refer to the activities of the corresponding species in mol L^{-1}, and K_1 and K_{CO_2}represent the first dissociation constants for CO_2 gas in water and the temperature-dependent Henry's Law, respectively. SI_C in a water body is calculated as:

$$SI_C = \lg\left(\frac{(Ca^{2+})(CO_3^{2-})}{K_C}\right) \quad (2)$$

where the species in parentheses is the ion activity product and K_C represents the temperature–dependent equilibrium constant of calcite dissolution. When SI_C>0, the water is supersaturated with respect to

calcite; when SI_C=0, the dissolution of calcite in the solution is in equilibrium; and when SI_C<0, the water is undersaturated with respect to calcite.

2.3. Lake metabolism on the diel scale

The methods used to measure the metabolism of aquatic ecosystems are increasingly diverse and have specific limitations and advantages. According to the methods and guidelines discussed by Winslow et al. (2016), continuous diel O_2 measurements are widely used to investigate lake metabolism (Odum, 1956; Cole et al., 2000; Demars et al., 2015; Hu et al., 2015; Winslow et al., 2016; Tonetta et al., 2016; Martinsen et al., 2017; Andersen et al., 2019; Herrera and Nadaoka, 2021). The change in DO in each time interval is caused by two processes: net ecosystem production, and diffusion exchange with the atmosphere. The following DO mass balance model was used to estimate the metabolic components of lakes, which is expressed as a bookkeeping model (Winslow et al., 2016):

$$\Delta DO = NEP_{t-1} \times \Delta t + F_{t-1} \tag{3}$$

Here, ΔDO is the change in the DO concentration over time (as O_2 in mg L^{-1} t^{-1}); and NEP (mg L^{-1} Δt^{-1}) is calculated as the mean of the time discrete NEP_t, attributing changes in DO between sequential observations (time elapsed=Δt) to NEP_t and discrete gas exchange. F_{t-1} (mg L^{-1}=g m^{-3}) refers to the gas exchange (as O_2) over a discrete period and is calculated as (Winslow et al., 2016):

$$F_t = \frac{K_t \times \Delta t}{Z_t} \times \left(O_{s,t} - DO_t\right) \tag{4}$$

where $O_{s,t}$ (mg L^{-1}) is the saturated oxygen concentration as a function of water temperature (T, kelvin) (Weiss, 1970), z_t is the mixed layer depth (m), and the coefficient k_t (m t^{-1}) is the diffusive oxygen exchange of gas with the atmosphere at a given temperature. k_t is estimated using the Schmidt coefficient (*Sc*) and the gas piston velocity corresponding to a Schmidt coefficient of 600 (k_{600}) (Tan et al., 2021):

$$k = K_{600} \times \left(\frac{S_C}{600}\right)^{-n} \tag{5}$$

where n is equal to 2/3 for the wind speed at 10 m height (U_{10}) <3.7 m s^{-1}, and 1/2 when U_{10} >3.7 m s^{-1}. Assuming a neutrally stable boundary layer, the gas exchange coefficient (k_{600}, *k* for a Schmidt number of 600, m t^{-1}) was estimated as a function of U_{10} from the equations of Cole and Caraco (1998):

$$K_{600} = 2.07 + \left(0.215 \times U_{10}^{1.7}\right) \tag{6}$$

$$U_{10} = U_h \times \left(1 + \frac{C_{d10}^{0.5}}{f \times \ln\left(\frac{10}{h}\right)}\right) \tag{7}$$

where U_h is the wind speed at the height of *h* m (m s^{-1}), $_{d10}$ is the drag coefficient at the height of 10 m (1.3×10^{-3}), and *f* is the Von Karman constant (0.4). With the listed constants, the following relationship is obtained (Tan et al., 2021):

$$U_{10} = 1.22 \times U_1 \tag{8}$$

The normalized k_{600} was calculated using an empirical relationship determined by the wind speed, and there is good correspondence between measured and predicted values (Crusius and Wanninkhof, 2003):

$$\text{for } U_{10} < 3.7\,\text{m s}^{-1};\ K_{600} = 0.72U_{10} \tag{9}$$

$$\text{for } U_{10} \geq 3.7\,\text{m s}^{-1};\ K_{600} = 4.33U_{10} - 13.3 \tag{10}$$

The Schmidt coefficient (*Sc*) is dependent on water temperature (°C, degree Celsius) and is calculated using the equation of Wanninkhof (1992):

$$S_C = 1800.6 - 120.1T + 3.7818T^2 - 0.0476T^3 \tag{11}$$

NEP_t is the balance between gross primary production (GPP_t) and respiration (R_t) at time t:

$$NEP_t = GPP_t - R_t \tag{12}$$

During the dark we assumed there was no photosynthesis (GPP_t=0), which enables us to estimate the average rate of O_2 respiration (R_μ, mg L^{-1} Δt^{-1}) from the discrete rates of NEP_t for all observations during the day (sunrise to sunset) (Winslow et al., 2016):

$$R_\mu = \frac{\sum_{i=1}^{n} \Delta DO_i - F_i}{x\ \Delta t} \tag{13}$$

where x is the number of nighttime observations. Total nighttime respiration (R_{night} (O_2 in mg L^{-1} d^{-1})) is calculated from x and R_μ. We assumed that R is constant throughout the 24 h period, and the total daytime respiration (R_{day}, mg L^{-1} d^{-1}) can similarly be calculated as the product of R_μ during the day (sunrise to sunset).

3. Results

3.1. Diel and seasonal variations of physicochemical parameters

The variation, average and timing of the diel cycles of the measured and calculated physicochemical parameters are summarized in Table 1. All four sampling surveys at sites LWH and JL were conducted under conditions of no rainfall. The duration of daylight changed from 10:44, 12:54, 13:22 and 11:16 h d^{-1} in January, April, July and October, respectively (Table 2). The persistent cloudy conditions in April resulted in the lowest total daily insolation (2543 W m^{-2} d^{-1}) during the four sampling periods, compared to January (5317 W m^{-2} d^{-1}) and July (7251 W m^{-2} d^{-1}), and October (5249 W m^{-2} d^{-1}). During the sampling period, the wind speed was low and its amplitude of variation was small, with the mean value decreasing from January (1.83 m s^{-1}) to October (1.13 m s^{-1}) (Table 2).

The charge balances, characterized by the normalized inorganic charge balance (NICB = 100 × ($TZ^+ - TZ^-$)/TZ^+, where $TZ^+ = K^+ + Na^+ + 2Ca^{2+} + 2Mg^{2+}$ and $TZ^- = HCO_3^- + Cl^- + NO_3^- + 2SO_4^{2-}$ in μEq (10^{-6} charge equivalent units per liter)) is generally within ±5%, which is acceptable (Li et al., 2011). In this study, samples showed an NICB of –3.4% (median) and –2.4% (mean), indicating that the contribution of organic acids and ligands to the charge balance was not significant. The diel cycles of T, pH, DO and SI_C were almost in phase and showed increasing trends during the day and decreasing trends at night. In contrast, EC, [Ca^{2+}],[HCO_3^-] and pCO_2 decreased during the day and began to increase at night (Figs. 2 and 3). The water temperature ranged from 14.7 °C to 26.8 °C, with the highest values during the afternoon (~13:00–16:00) and the lowest at around sunrise (~5:00–7:00). As for T, the lowest mean values of pH, SI_C, and DO were in January, and the largest amplitudes in the diel cycling of these parameters were in July. The coefficients of variation (CV) of pCO_2 in JL and LWH were 0.2–0.7 and 0.2–0.6, respectively, and the CV values of DO were 0.1–0.3, and 0.2–0.3, respectively (Table 2). The changes in the hydrochemistry at the two sites in different seasons were highly consistent. Similar values and trends of physicochemical changes were also found at different water depths of the water column (He et al., 2019), which indicates that the lake water was well mixed.

During the diel monitoring period in January and April of 2017, the $\delta^{13}C_{DIC}$ values were high during the day and low at night, but they showed a completely different trend in July and October: low values during the day and high values at night (Fig. 4). The magnitude of the diel variability of $\delta^{13}C_{DIC}$ at the two sites increased synchronously from January (JL, –1.22‰; LWH, –1.50‰) to April (JL, –0.23‰; LWH,

Table 1
Statistics on the diel variations in physicochemical parameters in Fuxian Lake in different seasons.

	January		April		July		October	
Sites	JL	LWHK	JL	LWHK	JL	LWHK	JL	LWHK
T /°C	15.0~16.7[a] (15.5)[b][0.0][c]	15.2~19.2 (15.5) [0.0]	15.2~17.9 (16.3) [0.0]	16.8~19.2 (17.5) [0.0]	21.9~26.7 (23.2) [0.0]	21.9~26.8 (23.9) [0.1]	19.6~21.7 (20.4) [0.0]	18.9~22.3 (20.3) [0.1]
pH	8.3~8.9 (8.5) [0.0]	8.2~9.3 (8.5) [0.0]	8.0~8.9 (8.5) [0.0]	8.2~9.1 (8.6) [0.0]	7.9~9.2 (8.6) [0.0]	8.7~9.4 (9.0) [0.0]	8.5~8.9 (8.7) [0.0]	8.9~9.1 (9.0) [0.0]
EC /(μs cm^{-1})	312~323 (319.3) [0.0]	310~325 (317) [0.0]	309~349 (320.5) [0.0]	300~323 (309.4) [0.0]	289~302 (290.8) [0.0]	279~305 (292.7) [0.0]	278~289 (282.5) [0.0]	280~288 (285.1) [0.0]
[Ca^{2+}] /(mg L^{-1})[d]	23.8~29.2 (27.4) [0.0]	24.8~30.5 (28.7) [0.0]	22.1~47.8 (29.5) [0.2]	19.6~37.2 (26.8) [0.2]	18.4~26.0 (22.4) [0.1]	19.4~22.7 (21.2) [0.0]	19.1~22.5 (20.4) [0.0]	17.7~22.0 (20.4) [0.0]
[HCO_3^-] /(mg L^{-1})[d]	169.7~210.9 (196.9) [0.1]	167.0~209.7 (196.1) [0.0]	190.8~226.7 (201.2) [0.0]	187.3~218.7 (200.2) [0.0]	174.2~195.4 (185.5) [0.0]	176.3~201.6 (190.0) [0.0]	157.3~225.5 (183.8) [0.1]	166.4~207.6 (191.9) [0.0]
SI_C	0.5~0.9 (0.6) [0.2]	0.4~1.2 (0.7) [0.3]	0.4~1.4 (0.7) [0.2]	0.4~1.0 (0.8) [0.2]	0.1~1.2 (0.7) [0.4]	0.8~1.3 (1.0) [0.1]	0.6~0.9 (0.7) [0.1]	0.9~1.1 (1.0) [0.1]
pCO_2 /Pa	18.5~95.9 (56.3) [0.4]	14.6~116.1 (67.9) [0.6]	19.5~166.3 (65.6) [0.5]	12.2~128.5 (45.0) [0.6]	8.1~222.8 (55.6) [0.7]	5.3~31.9 (17.3) [0.5]	18.0~47.6 (32.7) [0.2]	9.9~21.0 (16.1) [0.2]
DO /(mg L^{-1})	6.9~12.5 (8.1) [0.1]	5.2~13.3 (7.7) [0.3]	2.9~11.3 (7.9) [0.2]	3.5~10.7 (7.3) [0.2]	3.6~12.2 (6.8) [0.3]	5.7~16.3 (8.6) [0.3]	6.6~10.8 (8.0) [0.1]	6.0~8.9 (6.8) [0.1]
$\delta^{13}C_{DIC}$ /‰[e]	–1.8~–0.7 (–1.2) [0.3]	–2.5~0.3 (–1.5) [0.6]	–4.0~0.8 (–0.2) [5.7]	–2.3~0.9 (–0.1) [14.6]	–4.8~3.5 (–0.3) [8.6]	–1.1~2.3 (1.3) [0.7]	0.1~1.2 (0.8) [0.4]	–0.8~1.0 (0.1) [4.3]

[a] Minimum-maximum
[b] Mean values
[c] CV or variation coefficients = standard deviation / mean
[d] Calculated values from equations
[e] Analyzed value from an isotope sample

Table 2
Summary of the environmental conditions during the monitoring year of 2017 in Fuxian Lake.

Environmental conditions	Monitoring year of 2017			
	Winter (Jan. 17–18)	Spring (Apr. 21–23)	Summer (Jul. 27–29)	Autumn (Oct. 29–31)
Monitoring duration (h)	24	44	48	49
Time interval (min)	15	15	15	15
Daylight duration (h d^{-1})	10:44	12:54	13:22	11:16
Mean: solar radiation (W m^{-2} d^{-1})	5317	2543	7251	5249
Mean: wind speed (m s^{-1})	1.8	1.5	1.5	1.1
Mean: air temperature (°C)	12.6	15.3	22.2	12.2
Mean: precipitation (mm)	0	0	0	0

–0.07‰) to July (JL, –0.26‰; LWH, 1.30‰), following the same seasonal trend as the day length and water temperature.

3.2. Ecosystem metabolism

From January to July 2017, the variations of GPP (19–57 g O_2 m^{-2} d^{-1}) and R (9–54 g O_2 m^{-2} d^{-1}) were of a similar magnitude and varied approximately in parallel, increasing approximately twofold at both sites (Table 3). This likely reflects the increases in insolation, T and biomass, or the composition of aquatic organism assemblages. One reason for this is that aquatic plants are dominant in shallow lakes and experience high metabolic rates during July. The rates of GPP and R were higher at LWH than at JL, but they were closely correlated over time, which may indicate a common response to nutrient inputs as well as a well-mixed water body. Compared to other deeper and larger lakes (Hanson et al., 2003; Solomon et al., 2013), the rates of GPP and R in Fuxian Lake were relatively high and gave rise to substantial diel fluctuations in the rates of lake metabolism.

The balance between GPP and R (NEP) at the two sites was predominantly positive during the day and negative at night, in different seasons, except for one day in October at JL (–3.73 g O_2 m^{-2} d^{-1}) and for one day in April at LWH (–6.76 g O_2 m^{-2} d^{-1}). At Fuxian Lake, solar radiation could contribute to the diel cycle of heat content and be responsible for the changes in NEP in different seasons. However, the NEP in January was likely controlled mainly by the combined effects of solar radiation and wind. The wind speed exceeded 6 m s^{-1} on the morning of January 18th, intensifying the vertical heat transfer. NEP also showed diel variations with positive correlations with carbon cycling, including [HCO_3^-], pCO_2, SI_c and $\delta^{13}C_{DIC}$ (Figs. 5 and 6), which indicates that the NEP and carbon cycling were linked and controlled by common mechanisms.

4. Discussion

4.1. Origin of the diel variations in physicochemical and isotopic characteristics

In our previous study of the seasonal variation of physical and chemical variables within different depth profiles from the northern, central and southern parts of Fuxian Lake, throughout 2017, we concluded that these variations were controlled mainly by the metabolism of aquatic phototrophs (He et al., 2019). However, lake metabolism is poorly-quantified and little is known about it on the diel timescale. Streamflow and groundwater inputs, water temperature, gaseous exchange, carbonate precipitation and dissolution, and biological processes could be the main mechanisms responsible for the diel physicochemical characteristics of lake surface waters (Jiang et al., 2013; de Montety et al., 2011; Nimick et al., 2011; Liu et al., 2015; Yang et al., 2015; Chen et al., 2017; Pu et al., 2017; Siebers et al., 2020; Herrera and Nadaoka, 2021).

The effects of streamflow and groundwater inputs are considered to have negligible effects on the diel variability at sites LWH and JL, due to the small lake catchment area and strong buffering capacity of Fuxian Lake (He et al., 2019). According to previous monitoring data, little or no seasonal variations were observed in the physicochemical parameters of the groundwater, which show a steady trend. For instance, DO ranged

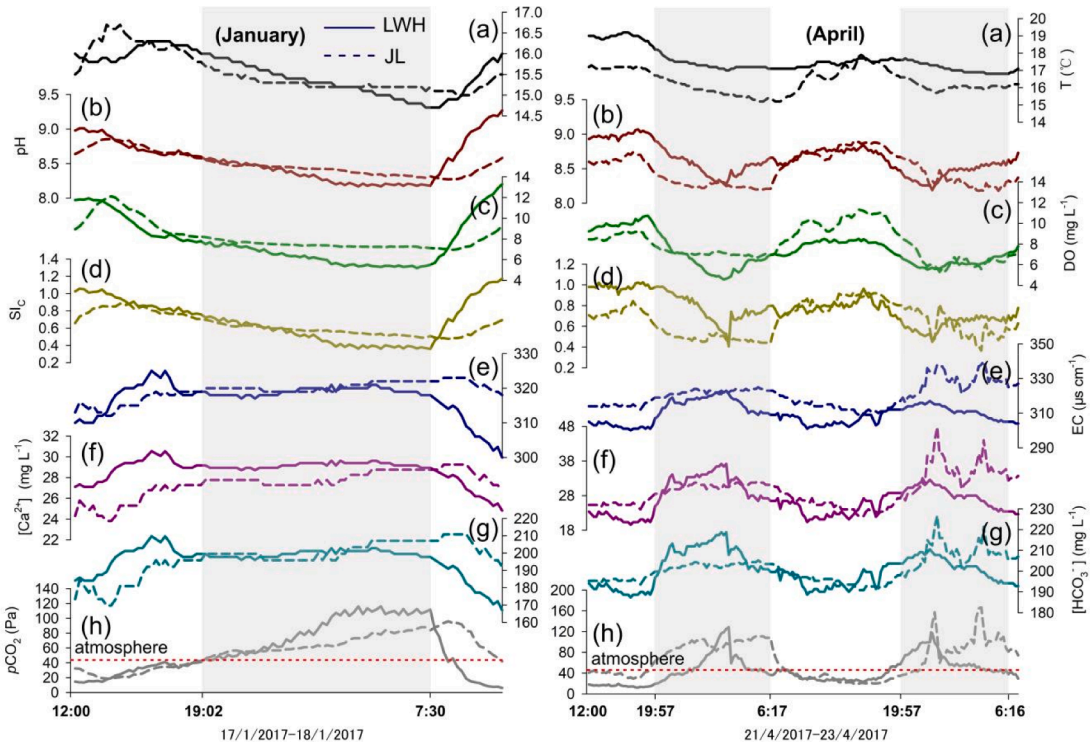

Fig. 2. Time series of (a) temperature, (b) pH, (c) DO (dissolved O_2), (d) SI_C (calcite saturation index), (e) EC (specific electronic conductivity), (f) $[Ca^{2+}]$, (g) $[HCO_3^-]$, and (h) pCO_2 during January (A) and April (B) at sites LWH and JL in Fuxian Lake. Red dashed line represents the CO_2 concentration in equilibrium with the atmosphere, and the grey shading represents the nighttime.

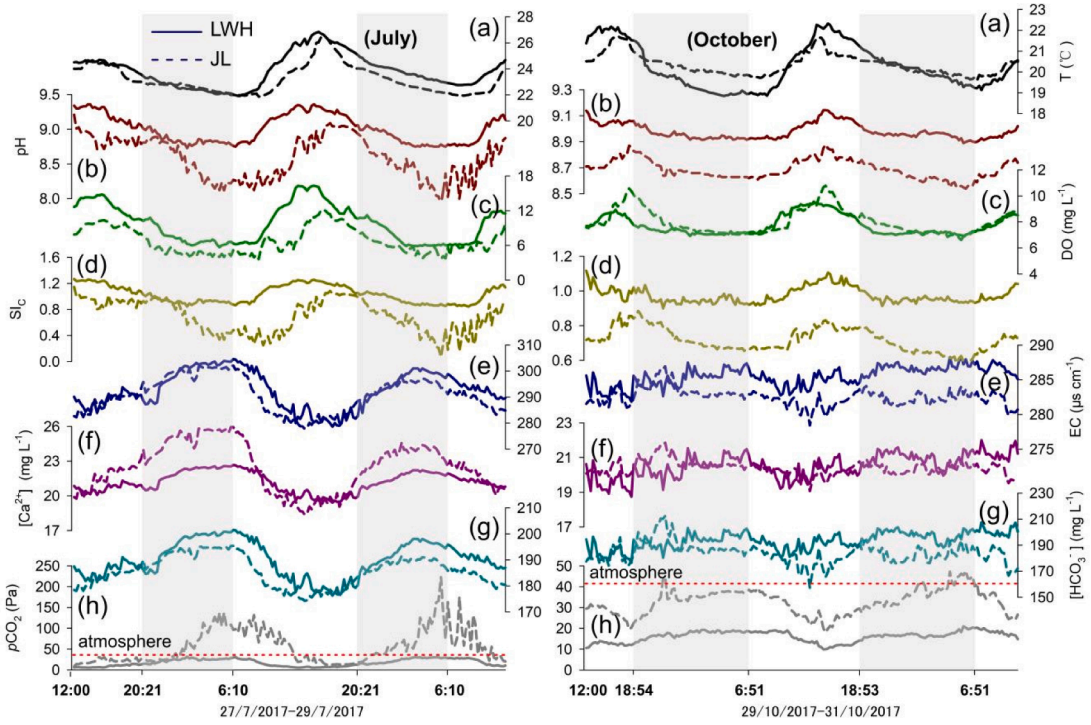

Fig. 3. Time series of (a) temperature, (b) pH, (c) DO (dissolved O_2), (d) SI_C (saturation index of calcite), (e) EC (specific electronic conductivity), (f) $[Ca^{2+}]$, (g) $[HCO_3^-]$, and (h) pCO_2 monitored in July (A) and October (B) at sites LWH and JL in Fuxian Lake. The red dashed line represents the CO_2 concentration in equilibrium with the atmosphere, and the grey shading represents the nighttime.

from 5.7 to 6.5 (6.2 on average) and was low and stable in different seasons (He et al., 2019), and significantly lower than the lake water. JL, especially, which is distant from major fluvial inputs, has the same diel characteristics as LWH; thus, external inputs were not the main driver of the physicochemical variations.

As noted in a comprehensive summary (Nimick et al., 2011), the

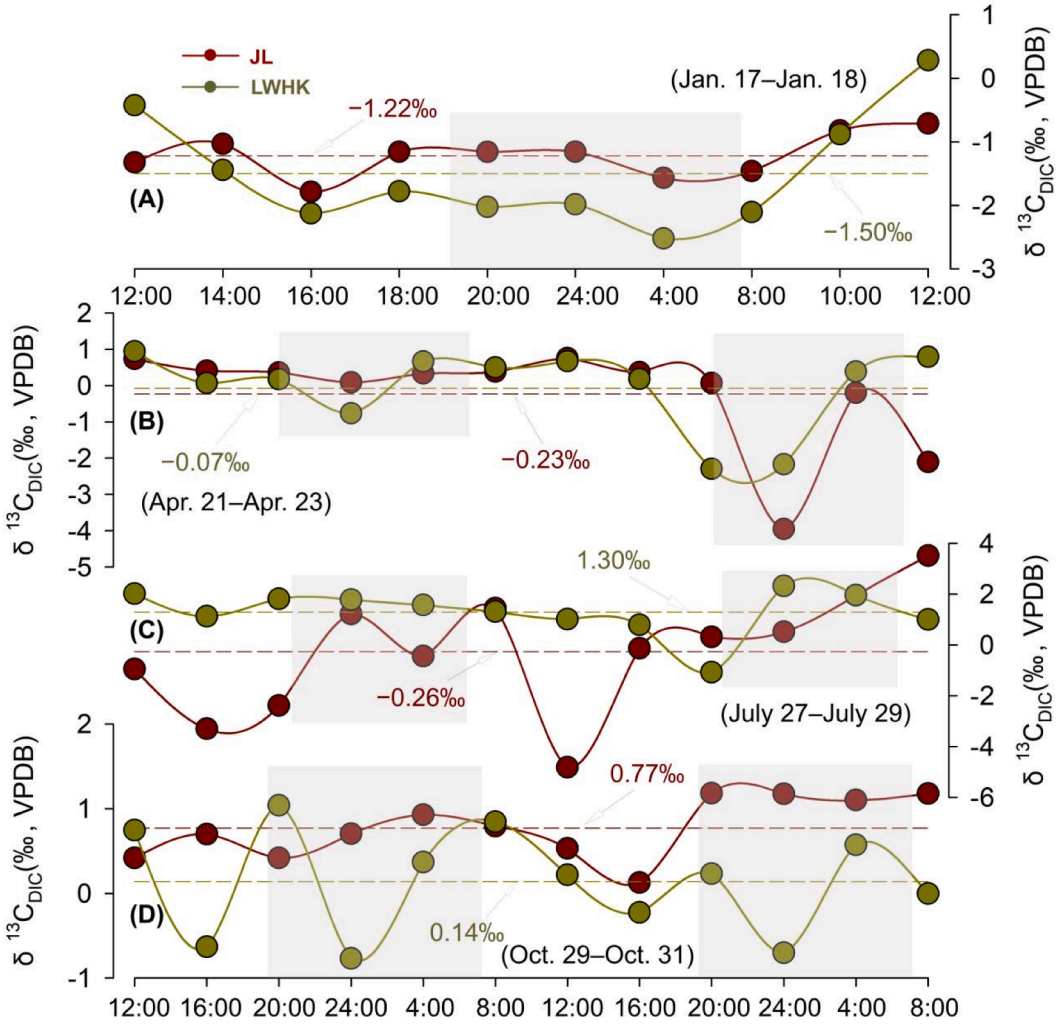

Fig. 4. Diurnal variations in $\delta^{13}C_{DIC}$ in January (A), April (B), July (C), and October (D) at sites JL and LWHK in Fuxian Lake. The dashed line represents the mean value. The grey shading represents nighttime.

Table 3
Summary of ecosystem metabolism during the monitoring year of 2017 in Fuxian Lake.

Sites	Ecosystem metabolism (g O_2 m^{-2} d^{-1})	Monitoring year of 2017			
		Winter (Jan. 17–18)	Spring (Apr. 21–23)	Summer (Jul. 27–29)	Autumn (Oct. 29–31)
LWH	GPP	38.6	5.2~9.1	27.3~48.3	6.1~12.0
	R	22.0	1.2~12.0	21.1~45.3	4.8~8.3
	NEP	16.6	–6.8~10.3	3.0~6.2	1.3~3.8
JL	GPP	19.2	17.3~27.6	28.0~30.9	13.8~16.0
	R	9.7	4.5~23.6	15.1~22.1	12.7~19.7
	NEP	9.5	4.0~12.8	8.8~12.9	–3.7~1.1

water temperature may show more consistent diurnal variability than other physicochemical properties. Temperature changes can affect the pH on the diel scale, either by changing the gaseous exchange rate between the water and atmosphere, or by changing the solubility of calcite (de Montety et al., 2011; Liu et al., 2015). It is noteworthy that less than 1% and 6% of the diel variations in pH and pCO_2, respectively, can be explained by water temperature changes, based on the hydrogeochemical simulation software PHREEQC. Additionally, although the changes in pCO_2 in the Fuxian Lake followed the temperature-solubility rule, the opposite trend in DO was observed (Fig. 7). This indicates that temperature was not the major control on the variations in pH, pCO_2 and DO on the diel timescale. Additionally, the influence of temperature on gaseous exchange is difficult to separate from that of biological processes, which are substantially driven by changes in solar radiation. Clearly, both mechanisms need to be considered together.

Gaseous exchange between air and water can induce variations in pCO_2 and DO (Nimick et al., 2011). Although it has been shown that inland lakes tend to be CO_2-supersaturated with respect to the atmosphere (Cole et al., 1994; Khan et al., 2020), the pCO_2 in Fuxian Lake was generally lower than that of the atmosphere, during the day (Figs. 2 and 3). Additionally, due to other processes, such as respiration by aquatic plants, CO_2 outgassing at night was not expected to have driven calcite precipitation (indeed, SI_c reached a minimum but remained positive) and to have enriched the $\delta^{13}C_{DIC}$ (indeed, a minimum value was attained) of the residual DIC (Fig. 4). Similarly, the results show relatively low and highly consistent k values of 2.7–4.2 cm h^{-1} for the O_2 diffusion coefficient across the air–water interface in different seasons. Also, as shown in Fig. 7, pCO_2 and DO were strongly negatively correlated, suggesting that degassing was not the major factor controlling pCO_2 and DO, as well as $\delta^{13}C_{DIC}$, on the diel timescale.

During the day, photosynthesis removes CO_2 (i.e., causing the depletion of ^{12}C in the remaining DIC) which thus increases the pH of the lake water and reduces the solubility of calcite, which may drive calcite precipitation (Liu et al., 2015). In most waters, biological activity

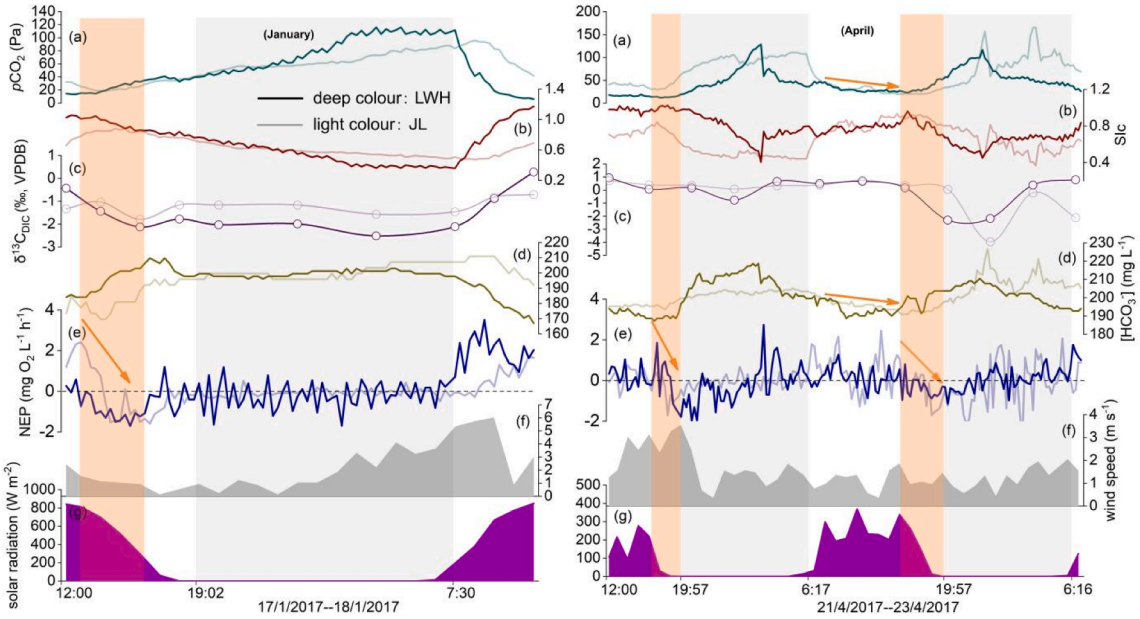

Fig. 5. Times series of (a) pCO_2, (b) SI_C, (c) $\delta^{13}C_{DIC}$, (d) [HCO_3^-], (e) NEP, (f) wind speed, and (g) solar radiation measured in January (A) and April (B) at sites LWH and JL in Fuxian Lake. The gray shading represents nighttime, and the orange shading represents the interval of rapid decline in NEP.

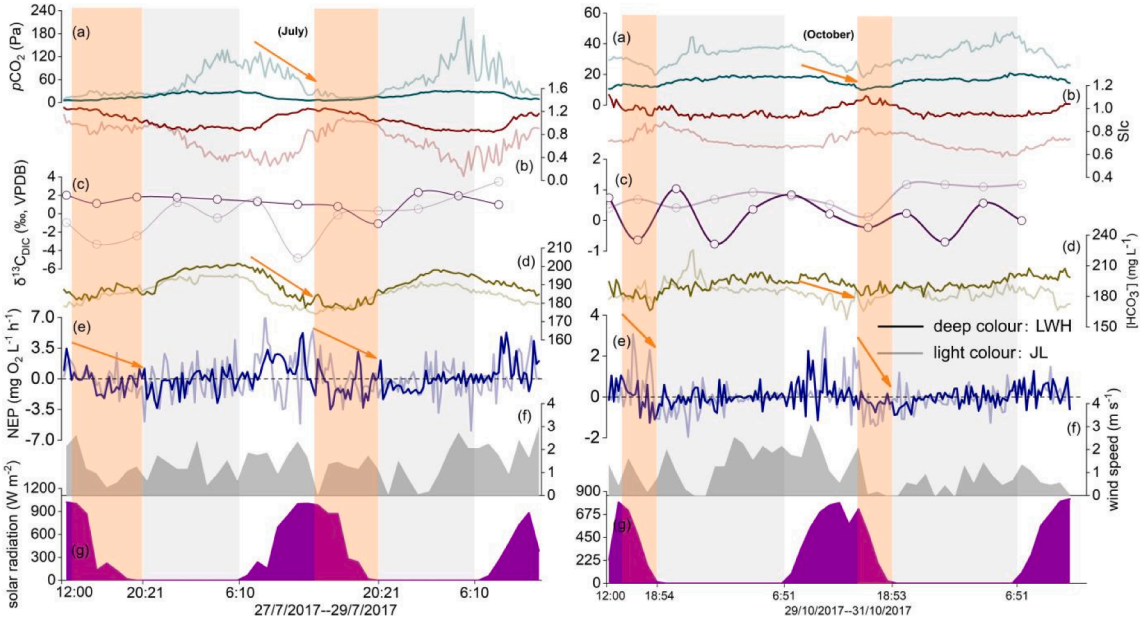

Fig. 6. Time series of (a) pCO_2, (b) SI_C, (c) $\delta^{13}C_{DIC}$, (d) [HCO_3^-], (e) NEP, (f) wind speed, and (g) solar radiation measured in July (A) and October (B) at sites LWH and JL in Fuxian Lake. The grey shading represents nighttime and the orange shading represents the period of rapid decline in NEP.

controls the CO_2 concentration which then influences the carbonate saturation (de Montety et al., 2011). In Fuxian Lake, SI_C generally increased to 1 during the day, and Ca^{2+} decreased linearly with HCO_3^- (Figs. 2 and 3), which suggests the potential for calcite precipitation to occur. Conversely, respiration at night increased the CO_2 concentration (i.e., releasing $^{12}CO_2$ into the water), decreased the pH, and thus promoted calcite dissolution. However, no carbonate dissolution occurred in Fuxian Lake during the monitoring period, because SI_C was always positive, indicating oversaturation with respect to calcite (Figs. 2 and 3) and the absence of carbonate dissolution at night. Therefore, carbonate dissolution is unlikely to have driven the changes in hydrochemistry and $\delta^{13}C_{DIC}$.

Several studies have shown that diel variations of pCO_2 and DO are induced by the photosynthesis and respiration of aquatic plants (e.g., Nimick et al., 2011; Liu et al., 2015; Yang et al., 2015; Chen et al., 2017; He et al., 2019). pCO_2 and DO follow opposite trends in Fuxian Lake (Fig. 7), coinciding with the metabolic processes operating in aquatic ecosystems. The diel variations of nutrients and DO, induced by biological activity, have also received attention (e.g., Odum, 1956; de Montety et al., 2011). During photosynthesis, the NO_3^- concentration decreases and the DO concentration increases, in response to the solar radiation level. These characteristics can be observed in Fuxian Lake; for example, NO_3^- was positively correlated with CO_2 (R^2=0.29) and negatively correlated with DO (R^2=0.26) at LWH in April. Additionally, when photosynthesis occurs during the day, $^{12}CO_2$ absorption by aquatic organisms occurs more rapidly than that of $^{13}CO_2$, generally resulting in

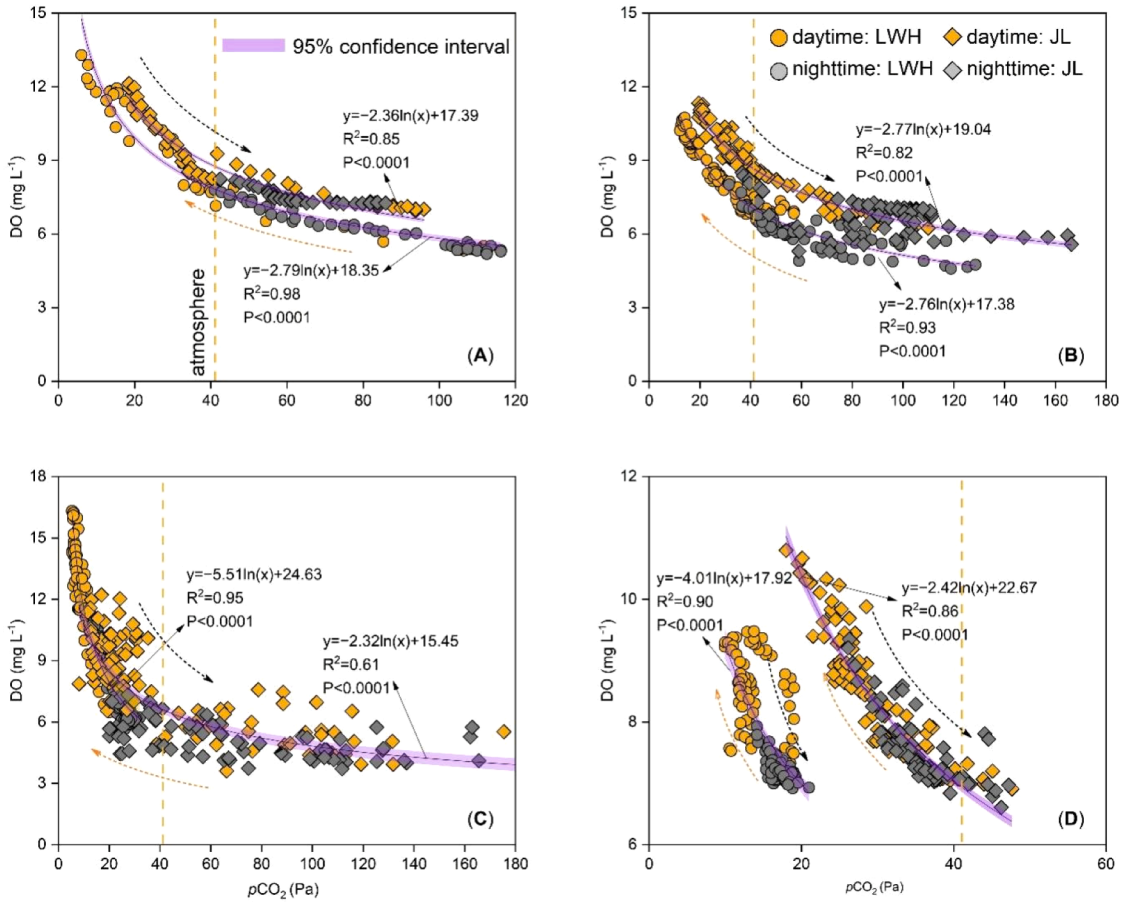

Fig. 7. Relationship between pCO_2 and DO in January (A), April (B), July (C), and October (D) at sites LWH and JL in Fuxian Lake. The black dashed arrows represent the trend of the changes during the night and the yellow dashed arrows represent the trend of changes during the day. The yellow dashed line represents the CO_2 concentration in equilibrium with the atmosphere.

enriched $\delta^{13}C_{DIC}$ values, which were observed in January and April 2017 (Fig. 4). In July and October, however, the opposite trend occurred (Fig. 4), which may be related to the strong degradation of organic matter (producing ^{13}C-depleted DIC) caused by the intensification of microbial activity (Parker et al., 2010), and/or the influx of atmospheric CO_2 and its kinetic fractionation (the isotope fractionation value can reach –13‰) (Herczeg and Fairbanks, 1987), which is clearly shown by the observation that the pCO_2 in July and October was lower than in April and January, and even lower than the atmospheric pCO_2 (Figs. 2 and 3). In general, more positive $\delta^{13}C_{DIC}$ values in the surface water occurred in July and October when most of the photosynthesis occurs. Overall, these observations emphasize the significant influence of biological metabolism on the hydrochemistry of Fuxian Lake.

4.2. *Lake metabolism and its influence on carbon dynamics*

The foregoing results confirm the existence of a diel cycle of aquatic metabolism (including aquatic photosynthesis and respiration) and its influence on the hydrochemistry and C isotopes of Fuxian Lake, as previously reported in both freshwater (Jiang et al., 2013; Liu et al., 2015; Yang et al., 2015; Chen et al., 2017; Pu et al., 2017; Siebers et al., 2020) and marine ecosystems (Teichert-Coddington and Green, 1993). The variations in these processes determine the fate of the carbon cycle in aquatic systems (Nimick et al., 2011; Staehr et al., 2012). Quantifying the rates of the production and degradation of aquatic plants and other organic matter is of fundamental importance for understanding the cycling of carbon and for estimating the status and maintaining the health of aquatic ecosystems (Castro et al., 2021). Recent investigations of metabolism via NEP in arctic, subarctic, temperate and tropical ecosystems have led to a better understanding of the contributions of aquatic ecosystems to carbon budgets, both regionally and globally (Bates and Mathis, 2009; Martinsen et al., 2017; Amaral et al., 2018; Andersen et al., 2019; Siebers et al., 2020; Herrera and Nadaoka, 2021). Our study of the littoral zone of Fuxian Lake, which has dense stands of submerged macrophytes, has documented the temporal and spatial changes of metabolic rates and carbon species, and we observed high rates and the close diel coupling of NEP and carbon species (Figs. 5 and 6). Although respiration always occurs and may even be higher during the day than at night, the gross primary production in Fuxian Lake exceeded the respiration (GPP>R; positive NEP), and aquatic plants consumed DIC (CO_{2aq}, HCO_3^-) and released O_2, causing increases in pH, SI_C and $\delta^{13}C_{DIC}$ (Fig. 8). Photosynthesis ceased at night and respiration was dominant (GPP<R; negative NEP), and aquatic plants consumed DO and released DIC, thereby reducing the pH, SI_C and $\delta^{13}C_{DIC}$ (Fig. 8). These observations indicate that the diel variations of the carbon cycle were largely controlled by the NEP.

The NEP was poorly correlated with wind speed on most occasions, while it was more strongly correlated with solar radiation and water temperature, which appears to be the main mechanism driving the changes in NEP. Especially in July (summer), the NEP reached a maximum under the high level of solar radiation and high water-temperatures (Figs. 5 and 6). Although high temperatures could intensify photorespiration and mitochondrial respiration even further (Kragh et al., 2017), as well as post-depositional mineralization rates (Gudasz et al., 2010), the increased primary productivity under the coupled effects of solar radiation and water temperature exceeded the effect of the increased respiration caused by temperature. This finding is consistent with observations in Lake Geneva (Castro et al., 2021), Capitol Lake

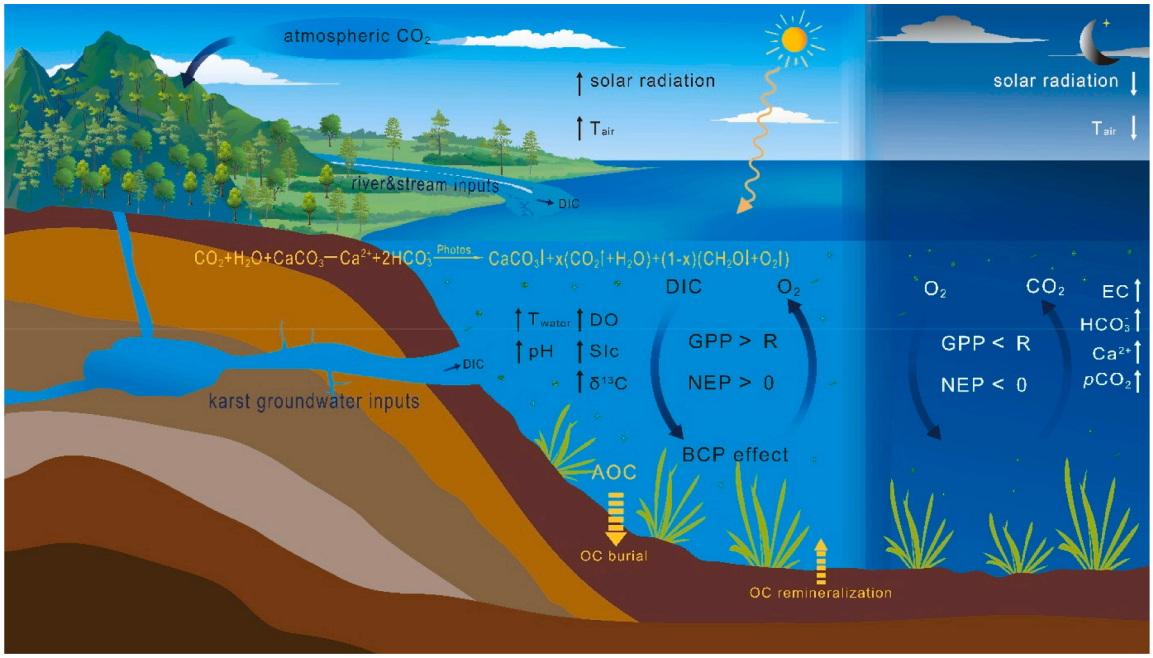

Fig. 8. Diagram illustrating how lake metabolic processes influence the physiochemical and isotopic properties and carbon cycling in Fuxian Lake. Carbonate weathering impacts carbon cycling by converting atmospheric CO_2 to bicarbonate ($CaCO_3+CO_2+H_2O \rightarrow Ca^{2+}+2HCO_3^-$), which is transported to lake ecosystems and is then partly consumed by aquatic phototrophs, driving the transformation from DIC (dissolved inorganic carbon) to AOC (autochthonous organic carbon) ($Ca^{2+}+2HCO_3^- \xrightarrow{\text{Photos.}} CaCO_3+x(CO_2+H_2O)+(1-x)(CH_2O+O_2)$), when the BCP (biological carbon pump) effect occurs (Liu et al., 2018). Thin arrows indicate increasing (↑) or decreasing (↓). DO=dissolved O_2. EC=specific electrical conductivity. pCO_2=CO_2 partial pressure. SI_C=calcite saturation index. $\delta^{13}C_{DIC}$=carbon isotopic compositions of DIC. GPP=gross primary production. R=ecosystem respiration. NEP=net ecosystem production.

(Yang et al., 2019), La Salada Lake, and Sauce Grande Lake (Alfonso et al., 2018), where solar radiation and water temperature were significantly positively correlated with the NEP. However, it contrasts with the case of Laguna Lake in the Philippines (Herrera and Nadaoka, 2021), which may be due to the absence of stable water column stratification in the rainy season. Indeed, multiple factors are likely responsible for the difference, as suggested by Herrera and Nadaoka (2021). For example, the biomass and physiological state of aquatic plants are not only affected by the water temperature, wind speed, and solar radiation, but also by the availability of inorganic nutrients, the structure of the food web, and the mixing regime.

Theoretically, the NEP is higher in the growing season, which is also the case at Fuxian Lake because of the strong solar radiation in summer and the flourishing of aquatic plants. Our paired DO–pCO_2 measurements support this viewpoint: i.e., DO reached a maximum of 16.31 mg L^{-1} and pCO_2 reached a minimum of 5.31 Pa during the monitoring period (Fig. 7). Additionally, during the summer productivity peak in shallow water, when CO_{2aq} depletion occurred (except for the influence of possible atmospheric CO_2 invasion, with corresponding depleted $\delta^{13}C_{DIC}$ values (Herczeg and Fairbanks, 1987), the HCO_3^- likely supports these high levels of GPP and NEP. Additionally, we found that in the afternoon of different seasons, pCO_2 and HCO_3^- varied synchronously, as did DO (Figs. 5 and 6). The DIC store in the form of HCO_3^- has developed two mechanisms to support GPP: (1) chemical exchange with CO_2 via hydration and ionization reactions, and (2) the CO_2 concentrating mechanism in submerged plants and algae (Aho et al., 2021). This may be why the GPP/R ratio in Fuxian Lake is higher than that of other lakes (Fig. 9), which likely indicates that karst lakes with high DIC support high primary production.

Positive NEP values were concentrated in the interval from sunrise to shortly after noon, while they were close to zero in the late afternoon and strongly negative at night, in all seasons. From morning to afternoon, solar radiation, T, DO and pH increased substantially, corresponding to decreased DIC (CO_{2aq}, HCO_3^-), which is likely the cause of the decrease in NEP at this time (Figs. 5 and 6). This is supported by *in situ* experiments, which showed that in water rich in DIC and with a hypoxic state, the photosynthesis of charophyte shoots cultured in surface water lacking DIC and dissolved oxygen was significantly reduced (Kragh et al., 2017). The littoral zone in Fuxian Lake is dominated by submerged plants which may have evolved CO_2 concentrating mechanisms (CCMs) that enable cells to increase the CO_2 concentration in cellular microcompartments to levels at which the carbon-fixing enzyme Rubisco can operate efficiently (Dülger et al., 2017). Due to the competitive interaction of the carboxylase and oxygenase activity of Rubisco, the CO_2/O_2 quotient at the site of activity is the result of the balance between photosynthetic CO_2 utilization and photorespiratory CO_2 depletion (Sand-Jensen and Frost-Christensen, 1998). Therefore, a lower DIC and higher oxygen concentration (lower DIC/DO and/or CO_{2aq}/DO) could limit photosynthesis in the late afternoon in Fuxian Lake (Figs. S1–S4). The low CO_2/O_2 ratio could also increase the photorespiration rate of aquatic plants, although the determination of the threshold needs further research.

4.3. Fuxian Lake as a net autotrophic ecosystem and its role as a metabolic sink for C

Understanding the balance of these metabolic processes is important because it defines the role of aquatic ecosystems in the global carbon cycle; that is, whether they are a source or sink of atmospheric carbon (Duarte and Agustí, 1998). In this study, we compared the GPP and R of aquatic communities to determine whether Fuxian Lake (hence potentially other lakes also) was a carbon source (GPP<R; NEP<0) or sink (GPP>R; NEP>0). Fig. 9 shows that R is associated with the ecosystem GPP, and the slope of the power equation is close to 1 (R^2=0.74; P<0.0001; n=14), which falls mainly within the field of lake aquatic ecosystems compiled by Hoellein et al. (2013). The NEP values in Fuxian Lake in July (summer) ranged from 3.0 to 12.9 g O_2 m^{-2} d^{-1}, with the mean value of 7.7 g O_2 m^{-2} d^{-1}; 25 globally distributed lakes had a

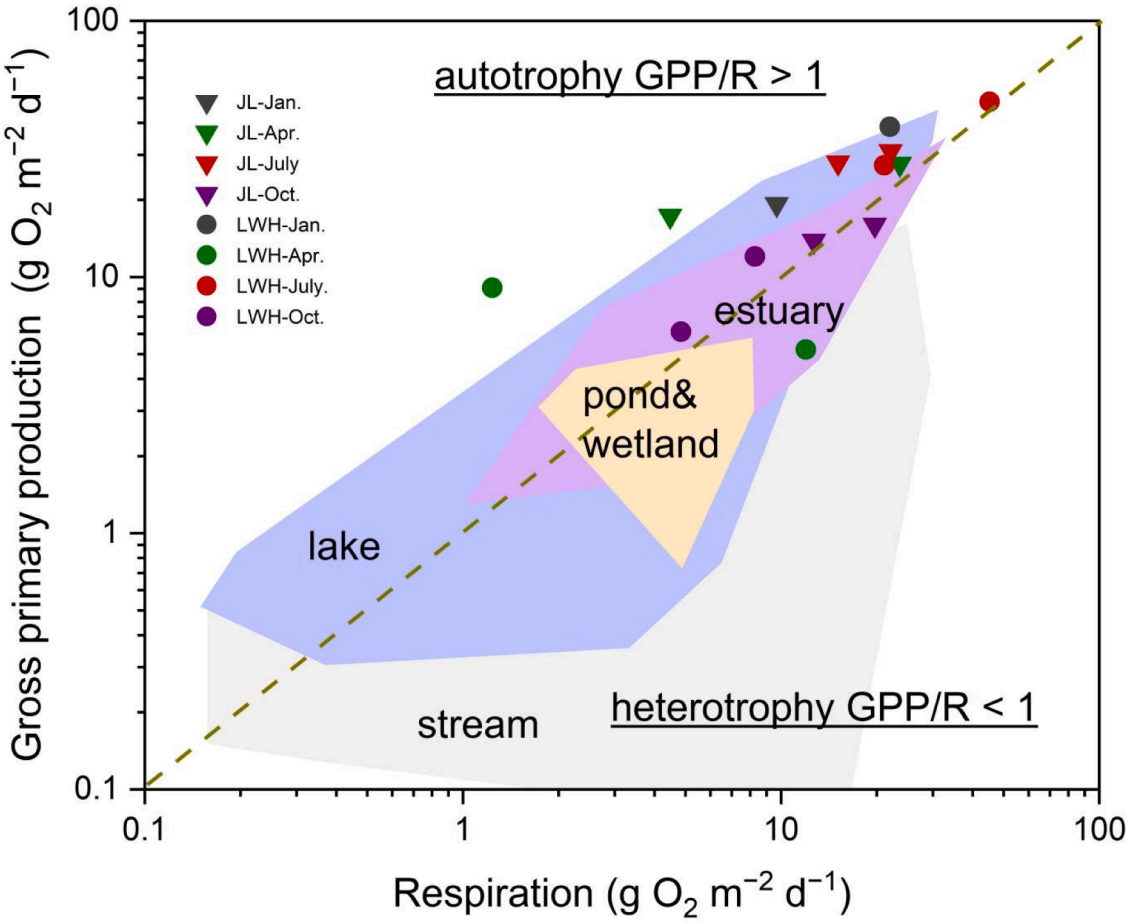

Fig. 9. Aquatic ecosystem metabolism showing GPP versus R for a data compilation from streams, lakes, ponds and wetlands, and estuaries (Hoellein et al., 2013). Filled triangles and circles are the daily rates of lake metabolism from measurements in January, April, July and October at sites JL and LWHK in Fuxian Lake. The dashed line represents the 1:1 value of GPP/R (Odum, 1956).

mean summer NEP value ranging from −7.3 to 9.9 g O_2 m^{-2} d^{-1}), as compiled by Solomon et al. (2013). Due to the small catchment area and long water retention time (167 years) of Fuxian Lake, the spatial heterogeneity of metabolism was low (Figs. 5, 6, and 9), indicating that the surface layer is well-mixed horizontally. Positive NEP values across the four seasons for the two monitoring sites (6.6 g O_2 m^{-2} d^{-1} on average) indicate that the lake ecosystem was net autotrophic and acted as a CO_2 sink.

To assess the potential atmospheric fluxes of C produced by lake metabolism in Fuxian Lake, GPP, R and NEP need to be converted to carbon units (g C m^{-2} a^{-1}). During photosynthesis, aquatic primary productivity consumes CO_2 and produces O_2 in the molar ratio (O_2/CO_2) of ~1.2 (Lefèvre and Merlivat, 2012; Aho et al., 2021). In contrast, the molar ratio of CO_2/O_2 for respiration with O_2 is 106/138 (Steinsberger et al., 2021). At the two monitoring sites in Fuxian Lake, the CO_2 sink flux by aquatic plants had the ranges of −0.7–345.7 g C m^{-2} d^{-1} at JL and 85.0–515.5 g C m^{-2} d^{-1} at LWH (obtained by calculation), with the corresponding fluxes of 902 t C km^{-2} yr^{-1} and 833 t C km^{-2} yr^{-1}, respectively, demonstrating an important potential CO_2 sink.

The metabolic organic carbon sink produced by the biological carbon pump (BCP) promotes the conversion from DIC to OC, and the magnitudes (833–902 t C km^{-2} yr^{-1}) in Fuxian Lake, a karst lake, are similar to our previous result estimated by ion (DIC, Ca^{2+}) mass balance at the epikarst aquatic photosynthesis rate (285–852 t C km^{-2} yr^{-1}; Liu et al., 2015; Yang et al., 2015), and is slightly higher than the Shawan Karst Test Site (156–493 t C km^{-2} yr^{-1} (Chen et al., 2017). These rates are ~25–81 times higher than that of the oceanic biological pump (Devries and Weber, 2017). Additionally, we found that at Fuxian Lake ~78% of inorganic carbon sources are photosynthetically fixed by aquatic plants in the form of HCO_3^-, based on a carbon isotope model (He and Li, 2021), from which the carbon sink flux can be seen to reach 650–704 t C km^{-2} yr^{-1}. These findings demonstrate the great potential of the combination of terrestrial aquatic photosynthesis and carbonate weathering for C sequestration. Therefore, atmospheric CO_2 uptake by the coupling of carbonate weathering with the aquatic photosynthesis mechanism should be considered within the regional and global carbon cycle and in climate models.

4.4. The role of karst lakes in the regional and global carbon cycle

Eutrophic aquatic ecosystems are generally regarded as a net CO_2 sink due to the high allochthonous inputs of inorganic nutrients (e.g., N, P) that could drive the conversion rate of DIC to OC (Michelle and John, 2011), whereas oligotrophic aquatic ecosystems act as a net CO_2 source and their primary productivity is controlled by cycling processes driven by heterotrophic organisms (Duarte and Agustí, 1998). On this basis, oligotrophic Fuxian Lake should be a heterotrophic lake. Although the metabolism monitoring in this study was not conducted in the center of the lake, net autotrophy is anticipated for Fuxian Lake considering the low organic supply from its small watershed and the deep-water environment, together with the fact that autochthonous organic carbon deposition occupies a dominant position (Chen et al., 2018; He et al., 2019, 2020). The NEP evaluation supports the notion that the shallow-water areas of large deep-water lakes are important components of global carbon processing, which is often overlooked. At the same time, the increasing eutrophication of such lakes will induce more

autochthonous deposition and, hence, CO_2 emissions to the atmosphere are expected to decrease (Liu et al., 2021; Ran et al., 2021).

The DIC (mainly HCO_3^-) utilization by aquatic plants, especially submerged plants (Dülger et al., 2017), is higher in karst lakes than in non-karst lakes (Liu et al., 2018). Liu et al. (2017) confirmed the conversion of DIC to autochthonous organic carbon (AOC) through ^{14}C analysis in the Pearl River Basin. Later, at the Karst Test Site (Chen et al., 2017; Bao et al., 2022) and in the Yangtze River and Yellow River (Liu et al., 2021; Zhao et al., 2022), the so-called "DIC fertilization effect" was identified in which more AOC% and phytoplankton biomass was produced with higher concentrations of DIC. Additionally, several studies identified a priming effect on the breakdown of both aquatic plants and terrestrially- derived C (Ward et al., 2016), which means that O_2 can be consumed by primary production and allochthonous organic matter in an aerobic environment; thus, a substantial part of the CO_2 emissions results from the degradation of allochthonous organic matter. Further, our research on karst aquatic ecosystems showed that chemoheterotrophy was significantly reduced in high DIC and Ca^{2+} environments, and that chemoheterotrophic planktonic bacteria were fewer, based on the dominant functional gene predicted by functional annotation of the prokaryotic taxa (Xia et al., 2022). Therefore, it is important to determine whether the influence of lake metabolism on the carbon cycle is specific to karst aquatic ecosystems.

Differences in the carbon budgets of karst lakes and non-karst lakes were also observed in several previous studies (Finlay et al., 2009; Tranvik et al., 2009). Karst lakes in the Northern Great Plains showed a net influx of CO_2 and efficient sediment storage (Finlay et al., 2009) relative to the non-karst lakes in the boreal catchment (Sobek et al., 2006). This difference could be explained by the simplified conceptual model shown in Fig. 10. Hard-water lakes, characterized by high pH and DIC but lower CO_2 concentrations, have been confirmed by statistical research on the global scale (Duarte et al., 2008). Coupled with the efficient utilization of DIC by aquatic plants, may further deplete dissolved CO_2. Additionally, AOC is resistant to microbial remineralization in high DIC and Ca^{2+} environments (Xia et al., 2022), which may also reduce CO_2 emissions and AOC storage. Thus, high AOC sedimentary storage and precipitated $CaCO_3$ were both observed in karst lakes in the Northern Great Plains (Finlay et al., 2009), which may confirm the occurrence of a strong BCP effect (Liu et al., 2018; He et al., 2020).

Finally, it is worth noting that the northern hardwater lakes shifted progressively from being substantial CO_2 sources in the mid-1990s to sequestering CO_2 by 2010, with increasing atmospheric warming and pH (Finlay et al., 2015). This decrease in CO_2 efflux may be due mainly to increasing aquatic photosynthesis (Liu et al., 2021). Additionally, HCO_3^- showed a steady trend of increase of 2.1–2.6% from 1950 to 2100, under a future climate and land-use scenario (Zeng et al., 2019). In the context of global climate change and lake eutrophication, a large amount of autochthonous production should, therefore, likely suffice to

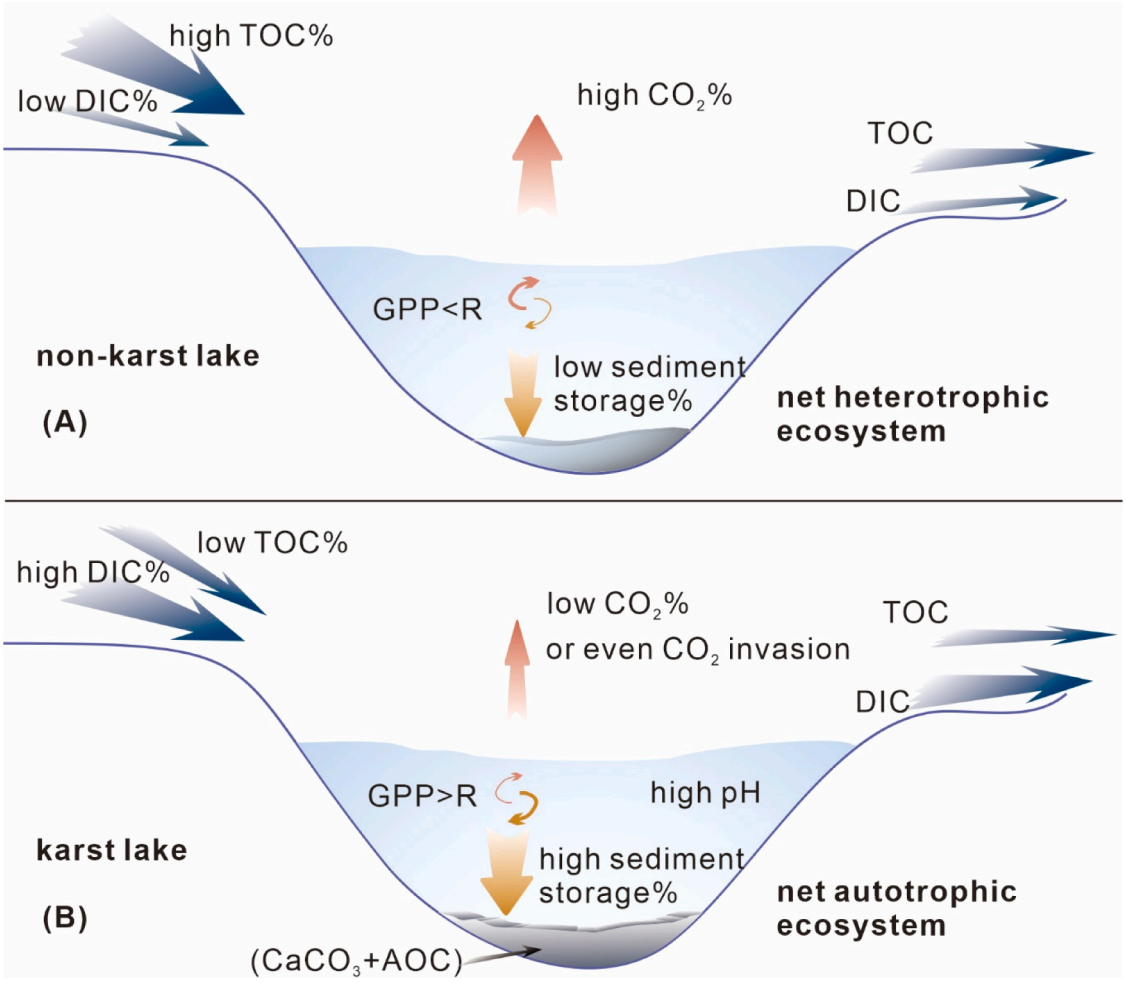

Fig. 10. Simplified conceptual diagram showing the difference in the carbon fluxes between a non-karst lake (A) and a karst lake (B), advancing the 'active pipe' concept presented by Cole et al. (2007) and Tranvik et al. (2009). The direction and width of the dashed arrows refer to the transfer process and magnitude respectively, which are summarized based on the currently available data (Sobek et al., 2006; Finlay et al., 2009, and this study). Lake environmental factors, such as basin lithology, form and concentration of C, and lake metabolic processes, will significantly affect the C dynamics, causing karst lakes to show different patterns of C fluxes compared to non-karst lakes.

drive aquatic ecosystems (especially the biota of karst aquatic ecosystems) towards net autotrophy, acting as a CO_2 sink. We recognize that such simple up-scaling has its limitations, and we also note that small continental waters should not be ignored in virtually all global processes and cycles (Downing, 2010; Williams et al., 2013; Holgerson, 2015; Holgerson and Raymond, 2016; Marcé et al., 2019), in which the processes and mechanisms of the carbon cycle, especially the impact of the differential contributions of autochthonous and allochthonous source, need to be clarified. Therefore, further research is needed to evaluate the importance of DIC-rich lakes in the magnitude and direction of C fluxes in the global C cycle.

5. Conclusions

Diel observations are crucial for understanding the biogeochemical cycling that governs subtropical lake aquatic ecosystems. The efficiency of the utilization by aquatic phototrophs of the dissolved inorganic carbon produced by carbonate weathering, is an important factor in determining the magnitude of the carbon sink, which can be estimated from diel observation of the hydrochemical and metabolism characteristics of surface waters.

Our monitoring of the diel variations of the hydrochemistry of Fuxian Lake revealed that it was controlled principally by the photosynthesis and respiration of aquatic communities, which is confirmed by quantitative metabolic parameters. The impact of lake metabolism on the lake carbon dynamics also reveals the importance of the biological carbon pump in supporting the high primary production in karst lakes. An additional discovery is that positive NEP values were concentrated during the interval from sunrise to shortly after noon, while they were close to zero in the late afternoon, in all seasons, which can be explained by the effects of the lower CO_2/O_2 ratio in limiting photosynthesis and increasing the potential for the photorespiration of aquatic plants. Fuxian Lake was found to be predominantly a net autotrophic ecosystem (GPP/R>1, NEP>0)—i.e., primary production exceeds respiration—suggesting that the lake functions more as a sink than a source of atmospheric carbon.

The estimated organic carbon sink produced by the metabolism of aquatic plants in Fuxian Lake reached 833–902 t C km^{-2} yr^{-1}, or around one order of magnitude higher than the oceanic biological pump. Combined with carbonate weathering the carbon sink flux will reach 650–704 t C km^{-2} yr^{-1}, indicating the crucial role of lacustrine aquatic photosynthesis in sequestering the carbon, caused by the coupling of carbonate weathering with aquatic photosynthesis.

Our findings demonstrate the importance of continuous monitoring on the diel scale in highly dynamic lake ecosystems. Additionally, they emphasize that the shallow water environment of deep-water lakes is an important component of global carbon processing that cannot be ignored, and that the inputs of large amounts of autochthonous organic carbon in karst aquatic systems have the ability to drive aquatic ecosystems towards net autotrophy and act as a CO_2 sink. Accordingly, future studies should incorporate better estimates of lake metabolism and their influence on carbon cycling to more fully evaluate the role of lakes, especially karst lakes, in regional and global carbon budgets.

Declaration of Competing Interest

The authors declare that they have no known competing financial interests or personal relationships that could have appeared to influence the work reported in this paper.

Acknowledgments

This study was financially supported by the National Natural Science Foundation of China (42141008, 42130501, 42007296, 41921004, 41977298), the Strategic Priority Research Program of the Chinese Academy of Science (XDB40020000), and the China Postdoctoral Science Foundation (2021T140582). We thank Jan Bloemendal for polishing the manuscript.

Supplementary materials

Supplementary material associated with this article can be found, in the online version, at doi:10.1016/j.watres.2022.118907.

References

Aho, K.S., Hosen, J.D., Logozzo, L.A., McGillis, W.R., Raymond, P.A., 2021. Highest rates of gross primary productivity maintained despite CO_2 depletion in a temperate river network. Limnol. Oceanogr. Lett. 6, 200–206.

Alfonso, M.B., Brendel, A.S., Vitale, A.J., Seitz, C., Piccolo, M.C., Perillo, G.M.E., 2018. Drivers of ecosystem metabolism in two managed shallow lakes with different salinity and trophic conditions: the Sauce Grande and La Salada Lakes (Argentina). Water 10, 1136.

Amaral, J.H.F., Borges, A.V., Melack, J.M., Sarmento, H., Barbosa, P.M., Kasper, D., de Melo, M.L., De Fex-Wolf, D., da Silva, J.S., Forsberg, B.R., 2018. Influence of plankton metabolism and mixing depth on CO_2 dynamics in an Amazon floodplain lake. Sci. Total Environ. 630, 1381–1393.

Andersen, M.R., Kragh, T., Martinsen, K.T., Kristensen, E., Sand-Jensen, K., 2019. The carbon pump supports high primary production in a shallow lake. Aquat. Sci. 81, 1–11.

Bao, Q., Liu, Z., Zhao, M., Hu, Y., Li, D., Han, C., Zeng, C., Chen, B., Wei, Y., Ma, S., Wu, Y., Zhang, Y., 2022. Role of carbon and nutrient exports from different land uses in the aquatic carbon sequestration and eutrophication process. Sci. Total Environ. 813, 151917.

Bates, N., Mathis, J., 2009. The Arctic Ocean marine carbon cycle: evaluation of air-sea CO_2 exchanges, ocean acidification impacts and potential feedbacks. Biogeosciences 6, 2433–2459.

Beerling, D.J., Kantzas, E.P., Lomas, M.R., Wade, P., Eufrasio, R.M., Renforth, P., Sarkar, B., Andrews, M.G., James, R.H., Pearce, C.R., Mercure, J.F., Pollitt, H., Holden, P.B., Edwards, N.R., Khanna, M., Koh, L., Quegan, S., Pidgeon, N.F., Janssens, I.A., Hansen, J., Banwart, S.A., 2020. Potential for large-scale CO_2 removal via enhanced rock weathering with croplands. Nature 583, 242–248.

Broecker, W.S., Takahashi, T., Simpson, H.J., Peng, T.H., 1979. Fate of fossil fuel carbon dioxide and the global carbon budget. Science 206, 409–418.

Castro, B.F., Chmiel, H.E., Minaudo, C., Krishna, S., Perolo, P., Rasconi, S., Wüest, A., 2021. Primary and net ecosystem production in a large lake diagnosed from high-resolution oxygen measurements. Water Resour. Res. 57 e2020WR029283.

Chen, B., Yang, R., Liu, Z., Sun, H., Yan, H., Zeng, Q., Zeng, S., Zeng, C., Zhao, M., 2017. Coupled control of land uses and aquatic biological processes on the diurnal hydrochemical variations in the five ponds at the Shawan Karst Test Site, China: implications for the carbonate weathering-related carbon sink. Chem. Geol. 456, 58–71.

Chen, B., Zhao, M., Yan, H., Yang, R., Li, H., Hammond, D.E., 2021. Tracing source and transformation of carbon in an epikarst spring-pond system by dual carbon isotopes (^{13}C-^{14}C): evidence of dissolved CO_2 uptake as a carbon sink. J. Hydrol. 593, 125766.

Chen, J., Yang, H., Zeng, Y., Guo, J., Song, Y., Ding, W., 2018. Combined use of radiocarbon and stable carbon isotope to constrain the sources and cycling of particulate organic carbon in a large freshwater lake. China. Sci. Total Environ. 625, 27–38.

Cole, J.J., Caraco, N.F., 1998. Atmospheric exchange of carbon dioxide in a low-wind oligotrophic lake measured by the addition of SF6. Limnol. Oceanogr. 43, 647–656.

Cole, J.J., Caraco, N.F., Kling, G.W., Kratz, T.K., 1994. Carbon dioxide supersaturation in the surface waters of lakes. Sci. New Ser. 265, 1568–1570.

Cole, J.J., Pace, M.L., Carpenter, S.R., Kitchell, J.F., 2000. Persistence of net heterotrophy in lakes during nutrient addition and food web manipulations. Limnol. Oceanogr. 45, 1718–1730.

Cole, J.J., Prairie, Y.T., Caraco, N.F., McDowell, W.H., Tranvik, L.J., Striegl, R.G., Duarte, C.M., Kortelainen, P., Downing, J.A., Middelburg, J.J., Melack, J., 2007. Plumbing the global carbon cycle: integrating inland waters into the terrestrial carbon budget. Ecosystems 10, 172–185.

Crusius, J., Wanninkhof, R., 2003. Gas transfer velocities measured at low wind speed over a lake. Limnol. Oceanogr. 48, 1010–1017.

de Montety, V., Martin, J., Cohen, M., Foster, C., Kurz, M., 2011. Influence of diel biogeochemical cycles on carbonate equilibrium in a karst river. Chem. Geol. 283, 31–43.

Demars, B.O., Thompson, J., Manson, J.R., 2015. Stream metabolism and the open diel oxygen method: principles, practice, and perspectives. Limnol. Oceanogr. Methods 13, 356–374.

Devries, T., Weber, T., 2017. The export and fate of organic matter in the ocean: new constraints from combining satellite and oceanographic tracer observations. Glob. Biogeochem. Cycles 31 (3), 535–555.

Downing, J.A., 2010. Emerging global role of small lakes and ponds: little things mean a lot. Limnetica 29 (1), 9–24.

Duarte, C.M., Agustí, S., 1998. The CO_2 balance of unproductive aquatic ecosystems. Science 281, 234–236.

Duarte, C.M., Prairie, Y.T., Montes, C., Cole, J.J., Striegl, R., Melack, J., Downing, J.A., 2008. CO_2 emissions from saline lakes: a global estimate of a surprisingly large flux. J. Geophys. Res. Biogeosci. 113, G04041.

Dülger, E., Heidbüchel, P., Schumann, T., Mettler-Altmann, T., Hussner, A., 2017. Interactive effects of nitrate concentrations and carbon dioxide on the stoichiometry, biomass allocation and growth rate of submerged aquatic plants. Freshw. Biol. 62, 1094–1104.
Finlay, K., Leavitt, P., Wissel, B., Prairie, Y., 2009. Regulation of spatial and temporal variability of carbon flux in six hard-water lakes of the northern Great Plains. Limnol. Oceanogr. 54, 2553–2564.
Finlay, K., Vogt, R.J., Bogard, M.J., Wissel, B., Tutolo, B.M., Simpson, G.L., Leavitt, P.R., 2015. Decrease in CO_2 efflux from northern hardwater lakes with increasing atmospheric warming. Nature 519, 215–218.
Gazeau, F., Gattuso, J.P., Middelburg, J.J., Brion, N., Schiettecatte, L.S., Frankignoulle, M., Borges, A.V., 2005. Planktonic and whole system metabolism in a nutrient-rich estuary (the Scheldt estuary). Estuaries 28, 868–883.
Goll, D.S., Ciais, P., Amann, T., Buermann, W., Chang, J., Eker, S., Hartmann, J., Janssens, I., Li, W., Obersteiner, M., 2021. Potential CO_2 removal from enhanced weathering by ecosystem responses to powdered rock. Nat. Geosci. 14, 545–549.
Gudasz, C., Bastviken, D., Steger, K., Premke, K., Sobek, S., Tranvik, L.J., 2010. Temperature-controlled organic carbon mineralization in lake sediments. Nature 466, 478. –U3.
Hanson, P.C., Bade, D.L., Carpenter, S.R., Kratz, T.K., 2003. Lake metabolism: relationships with dissolved organic carbon and phosphorus. Limnol. Oceanogr. 48, 1112–1119.
He, H., Li, X., 2021. Study on the utilization efficiency of HCO_3^- by aquatic plants and the buried flux of autochthonous organic carbon in Fuxian Lake (in Chinese). Quat. Sci. 41, 1140–1146.
He, H., Liu, G., Zou, Y., Li, X., Ji, M., Li, D., 2021a. Coupled action of rock weathering and aquatic photosynthesis: influence of the biological carbon pump effect on the sources and deposition of organic matter in Ngoring Lake, Qinghai Tibet Plateau, China. CATENA 203, 105370.
He, H., Liu, Z., Chen, C., Wei, Y., Bao, Q., Sun, H., Hu, Y., Yan, H., 2019. Influence of the biological carbon pump effect on the sources and deposition of organic matter in Fuxian Lake, a deep oligotrophic lake in southwest China. Acta Geochim. 38, 613–626.
He, H., Liu, Z., Chen, C., Wei, Y., Bao, Q., Sun, H., Yan, H., 2020. The sensitivity of the carbon sink by coupled carbonate weathering to climate and land-use changes: sediment records of the biological carbon pump effect in Fuxian Lake, Yunnan, China, during the past century. Sci. Total Environ. 720, 137539.
He, H., Liu, Z., Li, D., Zheng, H., Zhao, J., Chen, C., Bao, Q., Wei, Y., Sun, H., Yan, H., 2021b. Recent environmental changes in the Yunnan–Guizhou Plateau inferred from organic geochemical records from the sediments of Fuxian Lake. Elementa-Sci. Anthrop. 9, 1.
Herczeg, A.L., Fairbanks, R.G., 1987. Anomalous carbon isotope fractionation between atmospheric CO_2 and dissolved inorganic carbon induced by intense photosynthesis. Geochim. Cosmochim. Acta 51, 895–899.
Herrera, E.C., Nadaoka, K., 2021. Temporal dynamics and drivers of lake ecosystem metabolism using high resolution observations in a shallow, tropical, eutrophic lake (Laguna Lake, Philippines). J. Gt. Lakes Res. 47, 997–1020.
Hoellein, T.J., Bruesewitz, D.A., Richardson, D.C., 2013. Revisiting Odum (1956): a synthesis of aquatic ecosystem metabolism. Limnol. Oceanogr. 58, 2089–2100.
Holgerson, M.A., 2015. Drivers of carbon dioxide and methane supersaturation in small, temporary ponds. Biogeochemistry 124 (1), 305–318.
Holgerson, M.A., Raymond, P.A., 2016. Large contribution to inland water CO2 and CH4 emissions from very small ponds. Nat. Geosci. 9 (3), 222–226.
Hu, Z., Xiao, Q., Yang, J., Xiao, W., Wang, W., Liu, S., Lee, X., 2015. Temporal dynamics and drivers of ecosystem metabolism in a large subtropical shallow lake (lake Taihu). Int. J. Environ. Res. Public Health 12, 3691–3706.
Jiang, Y., Hu, Y., Schirmer, M., 2013. Biogeochemical controls on daily cycling of hydrochemistry and $\delta^{13}C$ of dissolved inorganic carbon in a karst spring-fed pool. J. Hydrol. 478, 157–168.
Khan, H., Laas, A., Marcé, R., Obrador, B., 2020. Major effects of alkalinity on the relationship between metabolism and dissolved inorganic carbon dynamics in lakes. Ecosystems 23, 1566–1580.
Kragh, T., Andersen, M.R., Sand-Jensen, K., 2017. Profound afternoon depression of ecosystem production and nighttime decline of respiration in a macrophyte-rich, shallow lake. Oecologia 185, 157–170.
Lefèvre, N., Merlivat, L., 2012. Carbon and oxygen net community production in the eastern tropical Atlantic estimated from a moored buoy. Glob. Biogeochem. Cycles 26, GB1009.
Li, X., Liu, Q., Liu, L., Liu, X., Bao, L., 2011. Identification of dissolved sulfate sources and the role of sulfuric acid in carbonate weathering using dual-isotopic data from the Jialing River, Southwest China. J. Asian Earth Sci. 42 (3), 370–380.
Li, Y., Wang, L., Qi, Y., Tang, F., 2007. Studies on the phytoplankton development trend in Lake Fuxian, China. J. Lake Sci. 19, 223–226.
Liu, H., Liu, Z., Macpherson, G., Yang, R., Chen, B., Sun, H., 2015. Diurnal hydrochemical variations in a karst spring and two ponds, Maolan Karst Experimental Site, China: biological pump effects. J. Hydrol. 522, 407–417.
Liu, Y., Wu, G., Gao, Z., 2008. Impacts of land-use change in Fuxian and Qilu basins of Yunnan Province on lake water quality. Chin. J. Ecol. 27, 447–453.
Liu, Z., Dreybrodt, W., Liu, H., 2011. Atmospheric CO_2 sink: silicate weathering or carbonate weathering? Appl. Geochem. 26, S292–S294.
Liu, Z., Dreybrodt, W., Wang, H., 2010. A new direction in effective accounting for the atmospheric CO_2 budget: considering the combined action of carbonate dissolution, the global water cycle and photosynthetic uptake of DIC by aquatic organisms. Earth Sci. Rev. 99, 162–172.
Liu, Z., Macpherson, G., Groves, C., Martin, J.B., Yuan, D., Zeng, S., 2018. Large and active CO_2 uptake by coupled carbonate weathering. Earth Sci. Rev. 182, 42–49.
Liu, Z., Yan, H., Zeng, S., 2021. Increasing autochthonous production in inland waters as a contributor to the missing carbon sink. Front. Earth Sci. 9, 620513.
Liu, Z., Zhao, M., Sun, H., Yang, R., Chen, B., Yang, M., Zeng, Q., Zeng, H., 2017. Old" carbon entering the South China Sea from the carbonate-rich Pearl River Basin: coupled action of carbonate weathering and aquatic photosynthesis. Appl. Geochem. 78, 96–104.
Marcé, R., Obrador, B., Gómez-Gener, L., Catalán, N., Koschorreck, M., Arce, M.I., Singer, G., von-Schiller, D., 2019. Emissions from dry inland waters are a blind spot in the global carbon cycle. Earth Sci. Rev. 188, 240–248.
Martinsen, K.T., Andersen, M.R., Kragh, T., Sand-Jensen, K., 2017. High rates and close diel coupling of primary production and ecosystem respiration in small, oligotrophic lakes. Aquat. Sci. 79, 995–1007.
Michelle, B., John, D., 2011. Carbon dioxide concentrations in eutrophic lakes: undersaturation implies atmospheric uptake. Inland Waters 1, 125–132.
Nimick, D.A., Gammons, C.H., Parker, S.R., 2011. Diel biogeochemical processes and their effect on the aqueous chemistry of streams: a review. Chem. Geol. 283, 3–17.
Odum, H.T., 1956. Primary production in flowing waters 1. Limnol. Oceanogr. 1, 102–117.
Parker, S.R., Gammons, C.H., Poulson, S.R., DeGrandpre, M.D., Weyer, C.L., Smith, M.G., Babcock, J.N., Oba, Y., 2010. Diel behavior of stable isotopes of dissolved oxygen and dissolved inorganic carbon in rivers over a range of trophic conditions, and in a mesocosm experiment. Chem. Geol. 269, 22–32.
Prairie, Y.T., Bird, D.F., Cole, J.J., 2002. The summer metabolic balance in the epilimnion of southeastern Quebec lakes. Limnol. Oceanogr. 47, 316–321.
Pu, J., Li, J., Khadka, M.B., Martin, J.B., Zhang, T., Yu, S., Yuan, D., 2017. In-stream metabolism and atmospheric carbon sequestration in a groundwater-fed karst stream. Sci. Total Environ. 579, 1343–1355.
Ran, L., Butman, D.E., Battin, T.J., Yang, X., Tian, M., Duvert, C., Hartmann, J., Geeraert, N., Liu, S., 2021. Substantial decrease in CO_2 emissions from Chinese inland waters due to global change. Nat. Commun. 12, 1–9.
Regnier, P., Friedlingstein, P., Ciais, P., Mackenzie, F.T., Gruber, N., Janssens, I.A., Laruelle, G.G., Lauerwald, R., Luyssaert, S., Andersson, A.J., Arndt, S., Arnosti, C., Borges, A.V., Dale, A.W., Gallego-Sala, A., Goddéris, Y., Goossens, N., Hartmann, J., Heinze, C., Ilyina, T., Joos, F., LaRowe, D.E., Leifeld, J., Meysman, F.J.R., Munhoven, G., Raymond, P.A., Spahni, R., Suntharalingam, P., Thullner, M., 2013. Anthropogenic perturbation of the carbon fluxes from land to ocean. Nat. Geosci. 6, 597–607.
Sand-Jensen, K., Frost-Christensen, H., 1998. Photosynthesis of amphibious and obligately submerged plants in CO_2-rich lowland streams. Oecologia 117, 31–39.
Siebers, A.R., Pettit, N.E., Skrzypek, G., Dogramaci, S., Grierson, P.F., 2020. Diel cycles of $\delta^{13}C_{DIC}$ and ecosystem metabolism in ephemeral dryland streams. Aquat. Sci. 82, 1–14.
Sobek, S., Söderbäck, B., Karlsson, S., Andersson, E., Brunberg, A.K., 2006. A carbon budget of a small humic lake: an example of the importance of lakes for organic matter cycling in boreal catchments. AMBIO J. Hum. Environ. 35, 469–475.
Solomon, C.T., Bruesewitz, D.A., Richardson, D.C., Rose, K.C., Van de Bogert, M.C., Hanson, P.C., Kratz, T.K., Larget, B., Adrian, R., Babin, B.L., 2013. Ecosystem respiration: drivers of daily variability and background respiration in lakes around the globe. Limnol. Oceanogr. 58, 849–866.
Staehr, P.A., Testa, J.M., Kemp, W.M., Cole, J.J., Sand-Jensen, K., Smith, S.V., 2012. The metabolism of aquatic ecosystems: history, applications, and future challenges. Aquat. Sci. 74, 15–29.
Steinsberger, T., Wüest, A., Müller, B., 2021. Net ecosystem production of lakes estimated from hypolimnetic organic carbon sinks. Water Resour. Res. 57 e2020WR029473.
Sun, H., Han, C., Liu, Z., Wei, Y., Ma, S., Bao, Q., Zhang, Y., Yan, H., 2022. Nutrient limitations on primary productivity and phosphorus removal by biological carbon pumps in dammed karst rivers: implications for eutrophication control. J. Hydrol. 607, 127480.
Tan, D., Li, Q., Wang, S., Yeager, K.M., Guo, M., Liu, K., Wang, Y., 2021. Diel variation of CH_4 emission fluxes in a small artificial lake: toward more accurate methods of observation. Sci. Total Environ. 784, 147146.
Teichert-Coddington, D.R., Green, B.W., 1993. Influence of daylight and incubation interval on water column respiration in tropical fish ponds. Hydrobiologia 250, 159–165.
Tonetta, D., Staehr, P.A., Schmitt, R., Petrucio, M.M., 2016. Physical conditions driving the spatial and temporal variability in aquatic metabolism of a subtropical coastal lake. Limnologica 58, 30–40.
Tranvik, L.J., Downing, J.A., Cotner, J.B., Loiselle, S.A., Striegl, R.G, Ballatore, T.J., et al., 2009. Lakes and reservoirs as regulators of carbon cycling and climate. Limnol. Oceanogr. 54, 2298–2314.
Wanninkhof, R., 1992. Relationship between wind speed and gas exchange over the ocean. J. Geophys. Res. Oceans 97, 7373–7382.
Ward, N.D., Bianchi, T.S., Sawakuchi, H.O., Gagne-Maynard, W., Cunha, A.C., Brito, D. C., Neu, V., de-Matos-Valerio, A., da Silva, R., Krusche, A.V., Richey, J.E., Keil, R.J., 2016. The reactivity of plant-derived organic matter and the potential importance of priming effects along the lower Amazon River. J. Geophys. Res. Biogeosci. 121, 1522–1539.
Weiss, R., 1970. The solubility of nitrogen, oxygen and argon in water and seawater. Deep Sea Research and Oceanographic Abstracts. Elsevier, pp. 721–735.
Williams, C.J., Frost, P.C., Xenopoulos, M.A., 2013. Beyond best management practices: pelagic biogeochemical dynamics in urban stormwater ponds. Ecol. Appl. 23 (6), 1384–1395.
Winslow, L.A., Zwart, J.A., Batt, R.D., Dugan, H.A., Woolway, R.I., Corman, J.R., Hanson, P.C., Read, J.S., 2016. LakeMetabolizer: an R package for estimating lake

metabolism from free-water oxygen using diverse statistical models. Inland Waters 6, 622–636.
Xia, F., Zhao, M., Li, Q., Li, D., Cao, W., Zeng, C., Hu, Y., Chen, B., Bao, Q., Zhang, Y., He, Q., Lai, C., He, X., Ma, Z., Han, Y., He, H., 2022. High stability of autochthonous dissolved organic matter in karst aquatic ecosystems: evidence from fluorescence. Water Res. 220, 118723.
Yang, R., Chen, B., Liu, H., Liu, Z., Yan, H., 2015. Carbon sequestration and decreased CO_2 emission caused by terrestrial aquatic photosynthesis: insights from diel hydrochemical variations in an epikarst spring and two spring-fed ponds in different seasons. Appl. Geochem. 63, 248–260.
Yang, R., Xu, Z., Liu, S., Xu, Y.J., 2019. Daily pCO_2 and CO_2 flux variations in a subtropical mesotrophic shallow lake. Water Res. 153, 29–38.
Zeng, S., Liu, Z., Groves, C., 2022. Large-scale CO_2 removal by enhanced carbonate weathering from changes in land-use practices. Earth Sci. Rev., 103915
Zeng, S., Liu, Z., Kaufmann, G., 2019. Sensitivity of the global carbonate weathering carbon-sink flux to climate and land-use changes. Nat. Commun. 10, 1–10.
Zhang, Y., Peng, T., Yu, J., Su, Y., Liu, Z., 2021. Natural and anthropogenically driven changes in the n-alkanols of lake sediments and implications for their use in paleoenvironmental studies of lakes. CATENA 207, 105591.
Zhao, M., Sun, H., Liu, Z., Bao, Q., Chen, B., Yang, M., Yan, H., Li, D., He, H., Wei, Y., Cai, G., 2022. Organic carbon source tracing and the BCP effect in the Yangtze River and the Yellow River: insights from hydrochemistry, carbon isotope, and lipid biomarker analyses. Sci. Total Environ. 812, 152429.